

Comparison of Geomatics Approach and Mathematical Model in Assessment of Soil Erosion Prone Areas – Kolli Hills, Namakkal District – Tamilnadu, India

Rajasimman Balasubramanian U.A.B., Gunasekaran S., Sakthivel G. and Saravanavel J.

Centre for Remote Sensing, Bharathidasan University, Khajamalai Campus, Tiruchirappalli, Tamilnadu, India

Correspondence should be addressed Rajasimman Balasubramanian U.A.B., to rajasimmanuab@hotmail.com

Publication Date: 1 June 2013

Article Link: <http://scientific.cloud-journals.com/index.php/IJAESE/article/view/Sci-20>



Copyright © 2013 Rajasimman Balasubramanian U.A.B, Gunasekaran S., Sakthivel G., and Saravanavel J. This is an open access article distributed under the **Creative Commons Attribution License**, which permits unrestricted use, distribution, and reproduction in any medium, provided the original work is properly cited.

Abstract Soil erosion assessment is a capital-intensive and time-consuming exercise. A number of parametric models have been developed to predict soil erosion prone zone at structural terrains, yet Universal Soil Loss Equation (USLE) is most widely used empirical equation for estimating annual soil Loss. While conventional methods yield point-based information, Remote Sensing (RS) technique makes it possible to measure hydrologic parameters on spatial scales while GIS integrates the spatial analytical functionality for spatially distributed data. Some of the inputs of the model such as cover factor and to a lesser extent supporting conservation practice factor and soil erodibility factor can also be successfully derived from remotely sensed data. In this study, Land sat ETM data was used to identify the land use status of Kolli hills region. Based on level of acquaintance effects of visual interpretation keys and through the digital image processing techniques the study region is classified into seven land use classes' namely wet crop, dry crop, fallow land, land with scrub and without scrub and water body. The base line studies were delineated from SOI Toposheet at 1:50,000 scale. A simple approach of rank sum method is tried to define the value of erosion risk prone zone areas in the study region then the assessment of soil erosion level in the study region is defined by applying USLE based approach. The modified LS factor map was generated from the slope and aspect map derived from the DEM. The K factor map was prepared from the soil map, which was obtained from the published soil map – by Soil Survey committee of geological survey of India. The P and C factor values were chosen based on the research findings of Central Soil and Water Conservation Research and Training Institute, Dehradun and spatial extent was introduced from land use/cover map prepared from Land sat ETM data. Maps covering each parameter (R, K, LS, C and P) were integrated to generate a composite map of erosion intensity based on the advanced GIS functionality. This intensity map was classified into different priority classes.

Keywords *RUSLE, Soil Erosion, GIS*

1. Introduction

Remote sensing provides convenient solution for this problem. Further, voluminous data gathered with the help of remote sensing techniques are better handled and utilized with the help of Geographical Information Systems (GIS). In this case study, GIS functionality were extensively utilized in the preparation of erosion and natural resources inventory and their analysis for assessing soil erosion and soil conservation planning. Scientific management of soil, water and vegetation resources on watershed basis is, very important to arrest erosion to retain the nutrient levels [6].

2. Objectives and Data Used

- To prepare the soil erosion prone area map using Remote Sensing and GIS techniques.
- Development of a soil erosion intensity map using modified universal soil loss equation with the aid of remotely sensed data in a GIS environment.
- Survey of India Toposheet: 58 I/7&8 on 1:50,000 scales.
- Landsat ETM (Nov 2006), Aster GDEM 30m and meteorological data–source www.IWMI.com/tools&resources/water%and%climate%atlas

3. Thematic Layers

3.1. Drainage and Lineament Density Map

Drainage is a major factor that contributes to soil erosion in hill areas. Both Drainage and soil erosion are reversely proportional to each other, soil erosion generally increases in well drained area and vice versa. In this study area, soil erosion is high near the drainage network when compared away from drainage; Terrain modification caused by gully erosion may also influence the initiation of Soil erosion. While, Lineaments are indirectly proportional to the standards of drainage impacts over soil erosion.

The drainage pattern is of dendritic at many locations because of dominant high peaks; it is influenced mainly by the joint pattern. From the prepared drainage map the density of drainage is assigned using ARC GIS – spatial analyst tools.

Table 1: Classification of Drainage and Lineament Density

Class	Drainage Density Value	Lineament Density Value
Very low	0-107.70	0-117.14
Low	107.70-215.41	117.14-234.29
Moderate	215.41-323.11	234.29-351.44
High	323.11-430.82	351.44-468.59
Very high	430.82-538.52	468.59-585.74

3.2. Geology

Table 2: Geological Succession of the Study Area

Symbol	Rock Type	Nature of Rock Type	Group	Age
HBG	Hornblende biotite gneisses	Metamorphic rock sediments	Peninsular gneisses complex	2,200-2550ma late archean to Proterozoic era
UB	Ultra mafic rocks	Hard rock sediments	Charnockites	2,600ma late archean era
CH	charnockites	Hard and easily weathered rocks		2,600ma archean era

3.3. Geomorphology of the Study Area

The prominent geomorphic units identified in Kolli hills through interpretation of Satellite imagery are 1) Erosional Plateau, 2) Composite slope, 3) Bazada zone, 4) Escarpment, 5) Intermountain Valley, 6) Pediments etc.

3.4. Landuse/Landcover

In this study supervised classification was employed to prepare the land use/ cover map of the study area. In this study, best results were obtained from maximum likelihood classifier. Using this classifier, the terrain was classified into seven land use/cover classes namely settlements, wet crop, dry crop, fallow land, dense forest, forest plantation, scrub forest, land with scrub, land with scrub, stony waste, river, tank ,etc. [1].

3.5. Slope Map

3.5.1. Imsd Slope Classification Based Slope Map

Aspect and altitude have bearing on vegetation type and conditions. Following the guidelines of all India soil and land use survey (AIS&LUS) on slope categories (void soil survey manual, IARI, 1971) slope map prepared on 1:50,000 scales.

Table 3: IMSD slope classifications

Slope Category	Slope (%)
Nearly level	0-1
Very gently sloping	1-3
Gently sloping	3-5
Moderately sloping	5-10
Strongly sloping	10-15
Moderately steep to steep sloping	15-35
Very steep sloping	>35

3.5.2. Active Passive Slope

Based on the level of vegetative cover the Active passive slope map was prepared from the satellite imagery.

3.6. Soil Map

Soil map are prepared from Tamilnadu soil map [Prepared and published by: National Bureau of Soil survey and Landuse Planning (ICAR) – Nagpur in association with Dept. Of Agriculture – Tamilnadu]. Their importance is taken as fact to discriminate their physical property [8].

3.6.1. Clayey Soils

Deep well drained clayey soils on moderately sloping high hill and hill ranges very severely clay soils on moderately sloping hill with moderate erosion.

3.6.2. Gravelly Clay Soil

Shallow well drained gravelly clay soil on gently sloping land moderately eroded associated with moderately shallow well drained gravelly clay soil.

3.6.3. Gravelly Loam Soils

Moderately shallow well drained gravelly clay soils on gentle sloping lands moderately eroded associated with shallow well drained gravelly loam soils.

3.6.4. Loamy Soils

Moderately shallow well drained loamy soils on gentle sloping lands moderately eroded.

3.6.5. Calcareous Loamy Soils

Moderately shallow well drained calcareous loamy soils on gently sloping low land moderately eroded associated with shallow well drained calcareous loamy soils.

3.6.6. Calcareous Cracking Clay Soils

Deep moderately well drained calcareous cracking clay soils on gently sloping lands moderately eroded associated with moderately well drained, calcareous cracking clay soils and slightly erosion .

4. Methodology

4.1. Rank Sum Method Analysis

Rank sum method analysis (RSMA) is a simple and calculation method for a combined analysis of multi class maps. A rank represents the relative importance of the parameter vise the objective. RSMA method takes into consideration of the parameter to calculate the each parameter.

$$\text{Rank sum method, } W_{ti} = \frac{K - r_i + 1}{\sum_{j=1}^K K - r_j + 1} \dots\dots\dots \text{(Equation - 1)}$$

Where, K- Total number of parameter; *r_i*- sub rank of parameter and *r_j*- total sub rank of parameter.

4.1.1. Assigning Weightages to the Parameters

Table 4: Assigning Weightages to Parameters in Root Sum Meth

SI. N	Parameter	Features	Rank	Straight Rank	K-ri+1	Wti	Wti%
1	Geomorphology	Erosional plateau	4	4.33	4.67	1.13	11.3
		Composite slope	3				
		Denudation hill	2				
		Escarpment	1				
		Intermountain valley	4				
		Bazada	5				
		Colluvial fan	7				
		Colluvial fill	7				
		Pediment	6				
2	Landuse/landcover	Land with scrub	6	4.28	4.72	2	20
		Scrub forest	6				

		Forest plantation	5				
		Dense forest	5				
		Dry crop	4				
		Fallow land	4				
		land without scrub	7				
		stony waste	4				
		Wet crop	3				
		Tank	1				
		River	2				
3	Active Passive	Active slope	2	1.5	7.5	1.38	13.8
		Passive slope	1				
4	Lithology	Ultramafic rock	1	2	7	1.2	12
		Charnockite	2				
		Fissile Hornblende	3				
5	IMSD classification slope	Plain	1	4	5	1.09	10.9
		Very gentle	2				
		Gentle	3				
		Moderate	4				
		Strong	5				
		Moderate to steep	6				
		Very steep	7				
6	soil	Severely eroded	3	2.18	6.82	1.2	12
		Moderately eroded	2				
		Slightly eroded	1				
7	Lineament density	Very low	1	3	6	1	10
		low	2				
		Moderate	3				
		Strong	4				
		High	5				
8	Drainage density	Very low	1	3	6	1	10
		Low	2				
		Moderate	3				
		Strong	4				
		High	5				
						SUM	100%

4.1.2. Assessment of Erosion Prone Zones

Final integration of Calculated Scores: $\text{Score} = \text{sub rank} * \text{Wti}$

Table 5: Calculated Score for Geomorphology

Geomorphology Feature	Sub Rank	Straight Rank	Wti	Score
Bazada	5			5.65
Colluvial fan	7			7.91
Colluvial fill	7			7.91
Composite slope	3			3.39
Denudation hill	2	4.33	1.13	2.26
Erosional plateau	4			4.52
Escarpment	1			1.13
Inter mountain valley	4			4.52
Pediment	6			6.78

Table 6: Calculated Score for Land Use and Landcover

Feature Type	Sub Rank	Straight Rank	Wti	Score
Dense forest	5			10
Dry crop	4			8
Fallow land	4			8
Forest plantation	5			10
Land with scrub	6			12
Land without scrub	7	4.28	2	14
River	2			4
Scrub forest	6			12
Stony waste	4			8
Tank	1			2
Wet crop	3			6

Table 7: Calculated Score for Lithology

Lithology Type	Sub Rank	Straight Rank	Wti	Score
Charnockite	2			2.4
Fissile hornblende biotite gneiss	3	2	1.2	3.6
Ultramafic rocks	1			1.2

Table 8: Calculated Score for Soil Type

Soil Description	Sub Rank	Straight Rank	Wti	Score	
Very deep- moderately well drained- calcareous loamy		1		1.2	
Very shallow- somewhat excessively drained- gravelly loam		3		3.6	
Shallow -well drained -gravelly loam		3		3.6	
Deep -moderately well drained- calcareous cracking clay		2		2.4	
Moderately shallow -well drained -gravelly clay		2		2.4	
Moderately shallow- well drained -loamy		2	2. 180	1.2	2.4
Deep -well drained- clayey		2		2.4	
Shallow- somewhat excessive drained- gravelly loam		3		3.6	
Shallow- well drained -gravelly clay		2		2.4	
Moderately deep -well drained- loamy		2		2.4	
Moderately shallow -well drained -calcareous loamy		2		2.4	

Table 9: Calculated Score for IMSD Slope Classification

Type of Slope	Sub Rank	Straight	Wti	Score
Moderate	4			4.36
Gentle	3			3.27
Moderate to steep	6			6.54
Plain	1	4	1.09	1.09
Strong	5			5.45
Very gentle	2			2.18
Very steep	7			7.63

Table 10: Calculated Score for Active / Passive Slope

Legend	Sub Rank	Straight	Wti	Score
Active slope	2	1.5	1.38	2.76
Passive slope	1			1.38

Table 11: Calculated Score for Lineament Density

Legend	Sub Rank	Straight Rank	Wti	Score
Moderate	3			3
Very low	1			1
Low	2	3.000	1	2
High	4			4
Very high	5			5

Table 12: Calculated Score for Drainage Density

Legend	Sub Rank	Straight Rank	Wti	Score
Moderate	3			3
Low	1			1
Very low	2	3.000	1	2
High	4			4
Very high	5			5

5. Determination of Factors of USLE

5.1. R-Factor

The rainfall erosivity map for each month was derived from the above equations which were implemented in “ArcGIS 9.3.1” software using the “Raster Calculator” tool of the “Spatial Analyst” extension (Figure 1) [4].

Table 13: Annual Precipitation Data for the Year 2011

Settlement	Jan	Feb	Mar	Apr	May	Jun	Jul	Aug	Sep	Oct	Nov	Dec
R.Pudupatti	1.84	0.84	5.22	31.96	73.99	39.8	68.83	98.19	108.94	171.69	82.4	33.35
Sirunavalur	3.28	0.67	3.94	27.26	56.27	24.71	34.64	76.11	105.28	174.49	100.35	43.95
Tattayangarpettai	3	0.67	3.57	29.99	56.54	22.82	35.85	72.26	100.61	173.41	92.17	39.27
Vairichetipalayam	2.61	0.77	5.35	27.95	65.62	28.6	42.68	87.42	112.44	174.19	98.28	42.29
Naganallur	2.61	0.77	5.35	27.95	65.62	28.6	42.68	87.42	112.44	174.19	98.28	42.29
Bellukkurichi	2.18	0.77	4.62	32.69	67.37	28.04	49.85	83.19	102.34	169.32	84.97	35.85
Erumaipatti	2.76	0.68	3.39	32.17	57.49	19.36	33.53	67.27	91.85	168.92	86.47	36.54
Namagiripettai	1.84	0.84	5.22	31.96	73.99	39.8	68.83	98.19	108.94	171.69	82.4	33.35
Pavitiram	3.07	0.7	2.83	33.71	53.24	10.71	20	52.56	78.18	160.2	85.33	39.1
Semmedu	2.46	0.84	5.57	31.86	69.78	28.31	49.63	87.65	118.03	172.91	99.31	47
Tammappatti	2.44	0.85	5.58	27.02	70.02	33.77	53.68	98.21	117.8	176.59	99.63	43.28
OsaikurayaUttaru	1.84	0.84	5.22	31.96	73.99	39.8	68.83	98.19	108.94	171.69	82.4	33.35
Periyakombai	2.15	0.87	5.71	30.42	74.11	34.84	59.31	96.27	120.25	174.94	95.33	42.94
Valakombai	2.46	0.84	5.57	31.86	69.78	28.31	49.63	87.65	118.03	172.91	99.31	47
Mangapatti	2.61	0.77	5.35	27.95	65.62	28.6	42.68	87.42	112.44	174.19	98.28	42.29

In USLE, the R-factor is derived from the following equation:

$$\log R = 1.93 \log \sum \left(\frac{P_i^2}{P} \right) - 1.52 \dots\dots\dots \text{(Equation – 2)}$$

Where, pi is monthly and P is the annual precipitation

Table 14: R-Factor Calculated from the Annual Precipitation Data

Settlement	Total	Mean	(Pi ² /P)-1.52	Log of (Pi ² /P)-1.52	R Factor
R.Pudupatti	717.05	59.75	8603.08	3.9347	7.5939
Sirunavalur	650.95	54.25	7809.88	3.8926	7.5128
Tattayangarpettai	630.16	52.51	7560.4	3.8785	7.4856
Vairichetipalayam	688.2	57.35	8256.88	3.9168	7.5595
Naganallur	688.2	57.35	8256.88	3.9168	7.5595
Bellukkurichi	661.19	55.10	7932.76	3.8994	7.5259
Erumaipatti	600.43	50.04	7203.64	3.8576	7.4451
Namagiripettai	717.05	59.75	8603.08	3.9347	7.5939
Pavitiram	539.63	44.97	6474.04	3.8112	7.3556
Semmedu	713.35	59.45	8558.68	3.9324	7.5895
Tammappatti	728.87	60.74	8744.92	3.9418	7.6076
OsaikurayaUttaru	717.05	59.75	8603.08	3.9347	7.5939
Periyakombai	737.14	61.43	8844.16	3.9467	7.6170
Valakombai	713.35	59.45	8558.68	3.9324	7.5895
Mangapatti	688.2	57.35	8256.88	3.9168	7.5595

5.2. K-Factor

The k-factor (soil erodibility factor) depends on the following soil parameters in combination:

- Percentage of silt, very fine sand, clay and organic matter.
- Structure (codes between 1 and 4 are given to different common structures).
- Drainage (codes between 1 and 6 are given from fast to very slow drainage).

Lal and Elliot in 1994 [7] proposed the following formula for k-erodibility factor calculation:

$$K=2.8*10^{-7}*M^{(1.14)} (1.2 - a) + 4.3*10^{-3}(b - 2) +3.3(c - 3)\dots\dots\dots \text{(Equation – 3)}$$

where M is the size of soil particles (% silt + % very fine sand)·(100 - % clay), a is the percentage of organic matter, b is the code number defining the soil structure (very fine granular = 1, fine granular = 2, coarse granular = 3, lattice or massive = 4), and c is the soil drainage class (fast = 1, fast to moderately fast = 2, moderately fast= 3, moderately fast to slow = 4, slow = 5, very slow = 6).

The K-Factor had calculated from the soil map published by - prepared and published by: National Bureau of Soil survey and Land use Planning (ICAR) – Nagpur in association with Dept. of Agriculture – Tamilnadu. (Figure 1).

Table 15: Calculated K Value for the Soil Type

Type	M	a	b	c	K - Factor
Calcareous loamy soil	10400	0.3	2	2	1.2
Gravelly Loam soil	7200	0.3	3	1	0.8
Calcareous cracking clay soil	3200	0.22	2	2	0.32
Gravelly clay soil	3200	0.3	3	2	0.32
Loamy soil	10400	0.3	2	2	1.2
Clayey soil	3200	0.26	1	2	0.32

Table 16: Textural Class and Corresponding Organic Content Level

Textural Class	O.M(avg)	O.M (<2%)	O.M (>2%)
Clay	0.22	0.24	0.21
Clay Loam	0.30	0.33	0.28
Coarse Sandy Loam	0.07	--	0.07
Fine Sand	0.08	0.09	0.06
Fine Sandy Loam	0.18	0.22	0.17
Heavy Clay	0.17	0.19	0.15
Loam	0.30	0.34	0.26
Loam fine sand	0.11	0.15	0.09
Loamy very fine sand	0.39	0.44	0.25
Sand	0.02	0.03	0.01
Sandy Clay loam	0.20	--	0.20
Sandy Loam	0.13	0.14	0.12
Silt Loam	0.38	0.41	0.37
Silty clay	0.26	0.27	0.26
Silty clay loam	0.32	0.35	0.30
Very fine sand	0.43	0.46	0.37
Very fine sandy loam	0.35	0.41	0.33

5.3. LS-Factor Calculation

The LS-factor map was derived from the DTM using the formula based on the work of (Moore, I and G. Burch, 1985) [10] for calculation of the S (slope steepness) and L (slope length) factors as follows: (Figure 1)

$$L = 1.4 * \left(\frac{AS}{22.13}\right)^{0.4} \dots\dots\dots(\text{Equation – 4})$$

$$S = \left(\frac{\sin\beta}{0.0896}\right)^{1.3} \dots\dots\dots(\text{Equation – 5})$$

Where AS: specific catchments area (m2/m), β: slope angle in degrees [11].

5.4. C-Factor Calculation

The C-factor represents how management affects soil loss. It is mainly related to the vegetation’s cover percentage and it is defined as the ratio of soil loss from specific crops to the equivalent loss from tilled, bare test-plots. The value of C depends on vegetation type, stage of growth and cover

percentage. For applications on national scale the C-factor can be estimated from mid-resolution satellite images by applying the Normalized Difference Vegetation Index (NDVI).

The NDVI was generated from satellite images (Landsat-7 ETM+) and the cell size was set at 100 × 100 m² (scale 1:100000). The NDVI value was estimated by the following equation: (Figure1)

$$NDVI = (NIR - IR) / (NIR + IR) \dots\dots\dots(\text{Equation} - 6)$$

Where NIR: the reflection of the near infrared portion of the electromagnetic spectrum and IR: the reflection in the upper visible spectrum. Since the original C-factor of USLE ranges from 0 (full cover) to 1 (bare land) and the NDVI values range from 1 (full cover) to 0 (bare land), the calculated NDVI values were inversed using “Raster Calculator” tool of the “Spatial Analyst” extension of “ArcGIS 9.3.1” software package. More specifically, the C-factor map was produced using the following exponential equation: [4, 9, 10].

$$C = \exp[-\alpha * (\frac{NDVI}{\beta - NDVI})] \dots\dots\dots(\text{Equation} - 7)$$

Where α , β : parameters determining the shape of the NDVI-C curve. A α -value of 2 and a β -value of 1 seem to give reasonable results.

5.5. P-Factor Calculation

The support practice factor P represents the effects of those practices that help prevent soil from eroding by reducing the rate of water runoff. The values of P are calculated as rates of soil loss caused by a specific support practice divided by the soil loss caused by row farming up and down the slope. In this work, however, the P-factor was taken as 1(ASD – 2001), since the study area is a structural terrain.

6. Soil Loss Tolerance Rate

A tolerable soil loss is the maximum annual amount of soil, which can be removed before the long term natural soil productivity is adversely affected [5]. The impact of erosion on a given soil type and hence the tolerance level varies, depending on the type and depth of soil. Generally, soils with deep, uniform, stone free topsoil materials and /or not previously eroded have been assumed to have a higher tolerance limit than soils which are shallow or previously eroded [3].

Correlative study of Erosion risk and Intensity of erosion:

- Since the study adheres a compact analysis of soil erosion risk analysis in the hill terrain an empirical approach of soil erosion intensity level is estimated which shows the region as a severe soil erosion risk prone zone. It is clearly procured that the level of intensity varies from 0.18 tons per hectare per year to 2,355 tons /ha/yr. Even though the value varies a large the relative study between the intensity level and erosion risk prone zone shows the distinct level of erosion intensity that matches with the land use land cover pattern of the area. (Figure 2)

The maximum level of erosion intensity in the study area is on ~227 ton/ha/yr. This value is defiantly matches with the zones that earned an accumulative score of 33.83 to 36.04 and are marked as high prior zones of Erosion risk.

Table 17: Soil Erosion Classes – Tolerance Value

Soil Erosion Class	Score Acquired in Rank Sum Analysis	Potential Soil Loss (tons/ha/year)	USLE Estimated Intensity (tons/ha/year)
Very Low	< 28.87	<5 (Tolerable)	0.8 – 3.5
Low	<31.57	5 – 10	7.87
Moderate	<36.58	10 – 15	15
High		15 – 25	22
Severe	<42	>25	31 - 92

Soil loss of up to 25 tons/ha/yr. is considered tolerable in mountainous areas where the natural rate of soil loss is high [10].

7. Conclusion

Soil losses are comparatively lower (less than 5 tons/ha/yr.) under land use types, such as Dense Forest, Wet crop cultivation areas. Annual soil loss rates are maximum (up to 92.37 tons/ha/yr.) in areas under present land use pattern. The moderate soil losses (< 15 tons/ha/yr.) are recorded in Scrub forest and Land with scrub regions.

In the forest plantation areas, Land with and without scrub and stony waste areas, soil losses vary from 31 to 92 tons /ha/yr. Furthermore from the present study it is concluded that

- The model was not data-demanding because it was fed only by data usually available in institutional databases, such as medium-high resolution satellite images, limited rainfall data (interpolated over the study area), geologic maps, etc.; in the same sense, the implementation was not expensive as well.
- The modified calculations of C and k-factors proved necessary and efficient, preparing the floor for further revisions and adaptations if appropriate.
- The model behaved better in agricultural areas confirming its original design to estimate long-term annual erosion rates in agricultural fields.

Figures

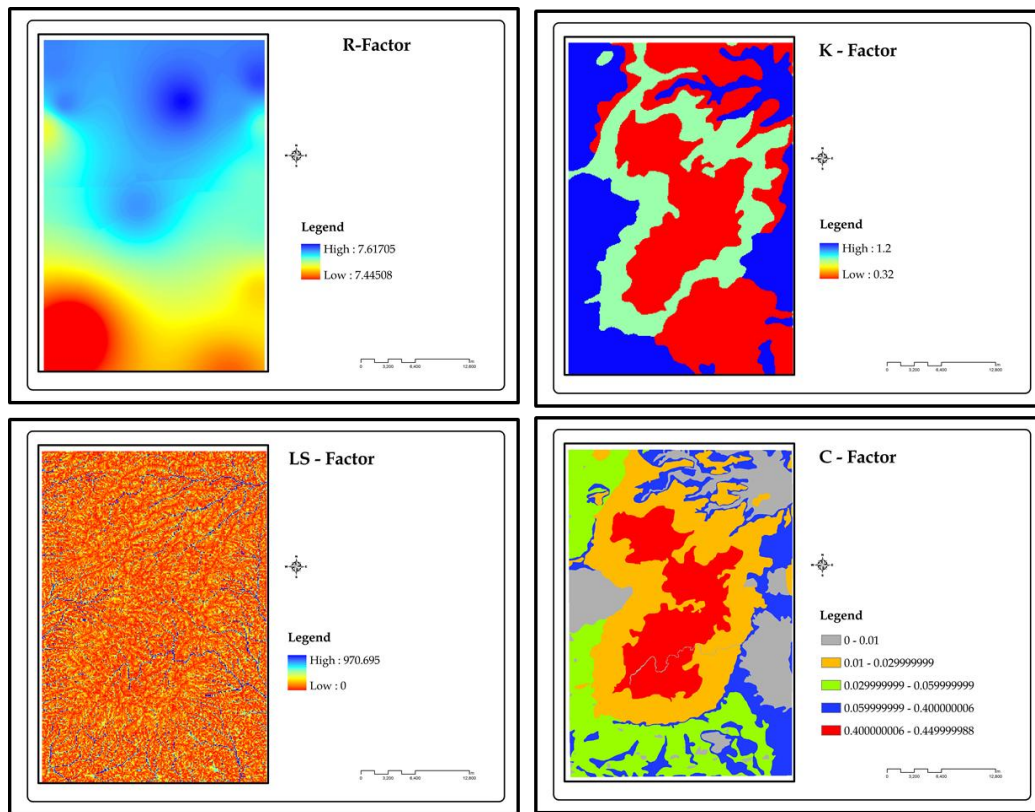


Figure 1: Estimated Values of USLE Parameters

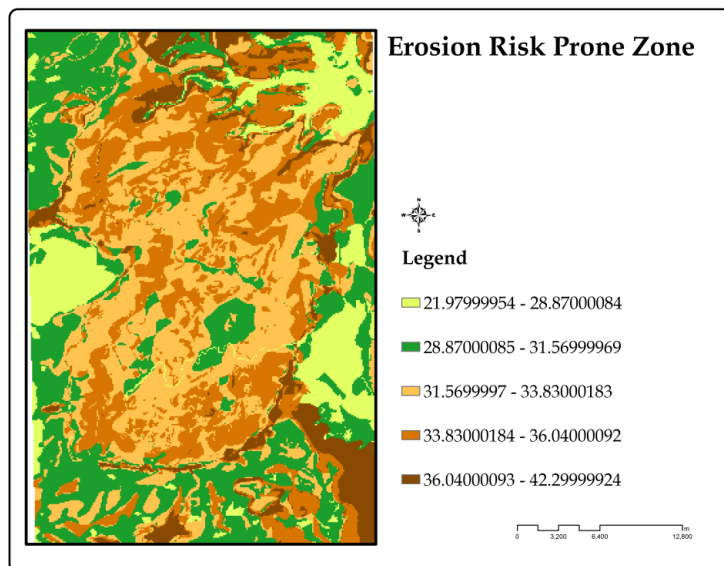


Figure 2: Root Sum Analyzed Classification of Soil Erosion Risk Prone Zones

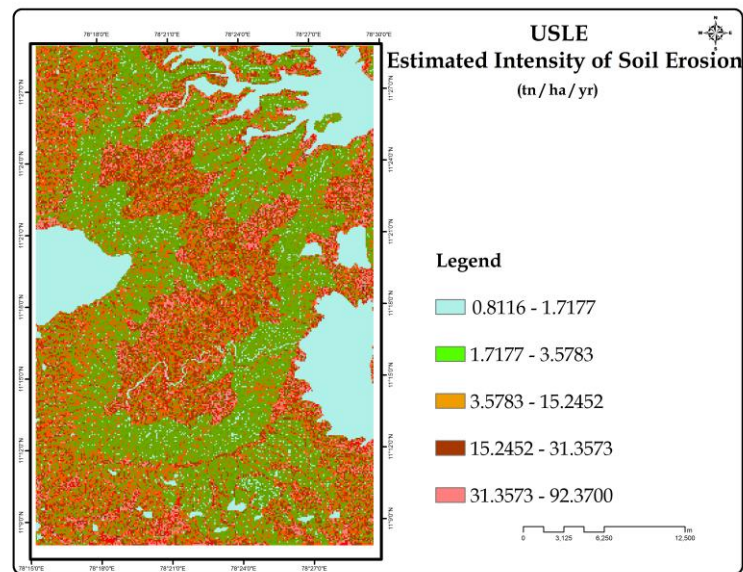


Figure 3: Estimated Soil Erosion Intensity Map – USLE Analysis

References

- [1] Agriculture & Soils Division, 2001: *IIRS P.G. Diploma Course Pilot Project Report On Land Evaluation for Landuse Planning By Integrated Use of Remote Sensing and GIS – A Case Study of Bhogabati Watershed in Kolhapur District.*
- [2] Gobin A. et al., 2002: *Second Annual Report of the Pan-European Soil Erosion Risk Assessment Project.*
- [3] Hikaru Kitahara et al. *Application of Universal Soil Loss Equation (USLE) to Mountainous Forests in Japan.* Journal for Remote Sensing. 2000. 5; 231-236.
- [4] Helena Mitsova et al. *Modeling Topographic Potential for Erosion and Deposition Using GIS.* International Journal of Geographical Information Systems. 2007. 10 (5) 629-641.
- [5] Lal R. *Soil Degradation by Erosion.* Land Degradation & Development. 2001. 12; 519- 539.
- [6] Lal R., et al., 1994: *Erodability and Erosivity.* Soil Erosion Research Methods. 2nd Ed. Soil and Water Conservation Society, 181-208.
- [7] Ioannis Z. Gitas et al., 2009: *Multi-Temporal Soil Erosion Risk Assessment in N. Chalkidiki Using a Modified USLE Raster Model.* EARSeL eProceedings, 8.
- [8] Manjul Kumar Hazarika et al., 1999: *Estimation of Soil Erosion Using Remote Sensing and GIS, Its Valuation and Economic Implications on Agricultural Production.* 10th International Soil Conservation Organization Meeting, Purdue University and the USDA-ARS National Soil Erosion Research Laboratory. 1090-1093.
- [9] Moore I., et al. *Physical Basis of the Length Slope Factor in the Universal Soil Loss Equation.* Soil Science Society of America Journal. 1985. 50; 1294-1298.

- [10]Morgan, 1985: *The Impact of Recreation on Mountain Soils: Towards A Predictive Model for Soil Erosion*. The Ecological Impacts of Outdoor Recreation on Mountain Areas in Europe and North America, Rural Ecology Research Group Report. 9; 112–121.
- [11]Pande L.M., et al., 1992: *Review of Remote Sensing Applications to Soils and Agriculture*. Proc. Silver Jubilee Seminar, IIRS, Dehra Dun.
- [12]Paolo Bazzoffi. *Soil Erosion Tolerance and Water Runoff Control: Minimum Environmental Standards*. Regional Environment Change. 2008. 9; 169–179.
- [13]Song Yang et al. *A Review of Soil Erodibility in Water and Wind Erosion Research*. Journal of Geographical Sciences. 2005. 15 (2) 167-176.
- [14]Van Remortel R., et al. *Estimating the LS Factor for RUSLE through Iterative Slope Length Processing of Digital Elevation Data*. Cartography. 2001. 30 (1) 27-35.
- [15]Wischmeier W.H., 1978: *Predicting Rainfall Erosion Losses - A Guide to Conservation Planning*. U.S. Department of Agriculture, Agriculture Handbook # 537.

Activity and Mass Concentration of ^{226}Ra , ^{228}Ra and ^{232}Th in Groundwater around the Zona Uranium Occurrence, Peta Gulf Syncline, Northeast Nigeria

A.S. Arabi¹, I.I. Funtua¹, B.B.M. Dewu¹, D.J. Adeyemo¹, J.D. Abafoni², M.L. Garba³ and I. Garba⁴

¹Centre for Energy Research and Training, Ahmadu Bello University, Zaria, Kaduna State, Nigeria

²Department of Physics, University of Maiduguri, Maiduguri, Borno State, Nigeria

³Department of Geology, Ahmadu Bello University, Zaria, Kaduna State, Nigeria

⁴Kano State University of Technology, Wudil, Kano State, Nigeria

Correspondence should be addressed to A.S. Arabi, saarabi@abu.edu.ng

Publication Date: 22 August 2013

Article Link: <http://scientific.cloud-journals.com/index.php/IJAESE/article/view/Sci-108>



Copyright © 2013 A.S. Arabi, I.I. Funtua, B.B.M. Dewu, D.J. Adeyemo, J.D. Abafoni, M.L. Garba and I. Garba. This is an open access article distributed under the **Creative Commons Attribution License**, which permits unrestricted use, distribution, and reproduction in any medium, provided the original work is properly cited.

Abstract In this study, eighteen groundwater samples were collected from wells in villages around Zona, an area reported to host uranium mineralization and these were analyzed for mass/activity concentration of ^{226}Ra , ^{228}Ra and ^{232}Th . Consumption of groundwater with elevated levels of ^{226}Ra , ^{228}Ra and ^{232}Th may result to cancer, kidney and/or developmental defects in humans and other animals. The results obtained were compared for compliance with international guidelines for radionuclides in drinking water. Results of the study showed that activity concentration of ^{226}Ra , ^{228}Ra and mass concentration of ^{232}Th ranged from 0.05 to 6.7pCi/L, 0.2 to 4.8pCi/L and 0.02 to 1.10 $\mu\text{g/L}$, respectively. The higher levels of ^{226}Ra in the studied samples compared with ^{228}Ra in same sample might be as a result of ^{226}Ra being part of ^{238}U decay series as a results of which ^{226}Ra is found over wide range of aquifer, it might also be an indication of secondary mineralization of uranium. Based on international guidelines regulating these radionuclides in groundwater, levels recorded at the time of the study fall within permissible limits of 20pCi/L for ^{226}Ra and ^{228}Ra while ^{232}Th which is insoluble in water, therefore, has no regulated limit. All radionuclides analyzed fall within international guideline despite occurrence of uranium mineralization in the study area.

Keywords Activity Mass Concentration, Radionuclides, Ionizing Radiation

1. Introduction

Regulating radionuclide levels in drinking water is gradually receiving global attention because of its health implications. In developing countries, the major health threat from water contamination has been bacterial and viral infection. However, for several decades now chemicals and radiological aspect of drinking water quality are receiving attention. Water can be radioactive due to the presence of naturally occurring radionuclides (NORs), which originates from the earth's crust, and are widely

distributed in the environment; in water, soils, rocks and air. Exposure to radioactivity increases the risk of various cancer cases to humans. Radon gas, Polonium, Lead and Bismuth increase the risk of lungs and stomach cancer, uranium and thorium increase toxicity risks to the kidneys and bones while radium increases the risk of bone cancer (bone sarcomas) and head carcinomas.

It is imperative to investigate the mass/activity concentration levels of these radionuclides in groundwater supply of the area because of the reported uranium occurrence. Because, once exposure is insured, it is not reversible; therefore, prevention is the best approach.

In this study, eighteen water samples were collected from wells in villages around Peta Gulf Syncline in the Upper Benue trough, northeastern Nigeria (Figure 1) and analyzed for mass/activity concentration of ^{226}Ra , ^{228}Ra and ^{232}Th . The results were compared for compliance with international guidelines for radionuclides in drinking water.

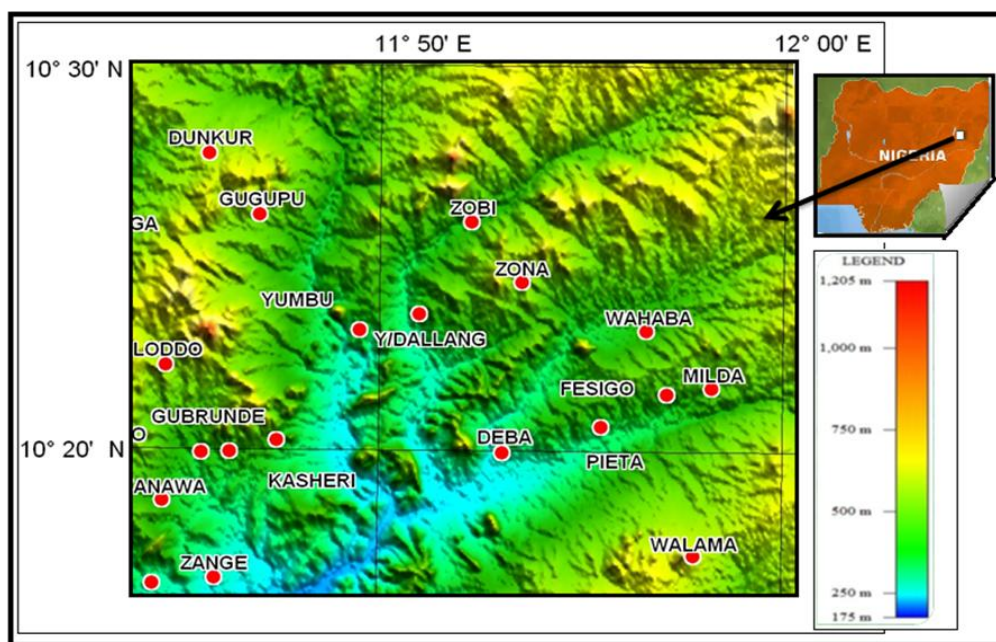


Figure 1: Digital Elevation Model of the Study Area Showing Sampled Points [Inset is a Map of Nigeria Showing Location of the Study Area (Globalmapper 13)]

The Peta Gulf Syncline is a fault bounded pull-apart sub-basin filled with the Bima Formation (Lower Cretaceous) which has three siliclastic members: (i) B₁: medial fan coarse-grained to micro-conglomeritic sandstones; (ii) B₂: full fluvial median-grained sandstones with minimal fines, and (iii) B₃: lacustrine and flood basin deposits comprising alternating fine-grained sand stone and siltstone/claystone (Suh *et al.*, 2000). According to Suh *et al.* (2000), the only significant uranium occurrence in the Peta Gulf Syncline is found around Zona (Zona uranium anomaly). Other localized mineralization around has been reported by Arabi *et al.* (2012), Elegba *et al.* (1993), Funtua *et al.* (1985; 1988; 1992; 1997) and Okujeni *et al.* (1987; 1990; 1994) around Gubrunde, Kanawa and Dali (all around the study area).

2. Materials and Methods

Groundwater samples were collected from eighteen hand dug wells, the dominant source of water for domestic activities in the area using standard procedure described in EPA water sampling protocol (EPA, 2004). The sites sampled were selected in a manner that covers all localities surrounding the entire areas reported to host uranium mineralization. In order to have a fresh sample from each well,

the well was purged for about fifteen minutes before sampling. The low density plastic bottles in which samples were collected were washed with distilled water followed by second washing with the sample before it was filled at a minimum flow. A sampling reproducibility test was performed *in-situ* by measuring five successive samples from same site and the results showed no deviation. Procedures adopted for analysis of Radium and Thorium is detailed in Eichrom procedures (Eichrom, 2006; Moon et al., 2003).

The test method is based on the utilization of solid phase extraction of radium from water samples. The detection of the ^{226}Ra is by alpha spectrometry and ^{228}Ra via ^{228}Ac by gas flow proportional beta counter.

An aliquot of the sample is measured into a beaker; barium carrier and ^{133}Ba were added. Radium and Barium were sorbed on an ion exchange column, eluted, evaporated to dryness, and dissolved in 0.095M HNO_3 . The dissolved solution was loaded on solid phase extraction column. ^{228}Ac was selectively sorbed on a solid phase extraction column, while ^{226}Ra and ^{133}Ba passed through the column. ^{228}Ac was eluted with 0.35M HNO_3 , and is precipitated with cerium fluoride. The precipitate was collected on a filter paper and counted for beta radiation. ^{226}Ra and ^{133}Ba were collected and precipitated with barium sulfate. The precipitate was collected on a filter. ^{133}Ba was counted using a gamma counter while Ra-226 is counted via alpha spectrometry.

The relation given below was used to calculate ^{228}Ra activity:

$$^{228}\text{Ra} \text{ (pCi/L)} = \frac{A}{2.22 \times E \times V \times Y \times e^{-\lambda t_2}} \times \frac{\lambda t_2}{1 - e^{-\lambda t_2}}$$

Where:

A = Net count rate, cpm

E = Counting efficiency expressed as fraction

Y = ^{133}Ba (Ra) yield expressed as fraction

V = Sample volume (liters)

t_1 = Decay time of ^{228}Ac , from start of rinse until start of counting (minutes)

t_2 = Counting time (minutes)

λ = Decay constant of ^{228}Ac ($1.88 \times 10^{-3} \text{ min}^{-1}$)

While for ^{226}Ra activity, the relation given below was used

$$^{226}\text{Ra} \text{ (pCi/L)} = \frac{S - B}{2.22 \times E \times V \times Y}$$

Where:

S = Sample counts per minute

B = Background counts per minute

E = Efficiency of counter

V = Volume of samples in liters

Y = $^{133}\text{Barium}$ yield.

Thorium was separated from uranium by Eichrom resins (Horwitz, E.P., 1993; Horwitz, E.P., 1992; Kressin, I.K., 1977; Maxwell, S.L., 1993; Nelson, D., 1992) prior to measurement by alpha Spectrometry as described in Eichrom, 2001. A calcium phosphate precipitation technique was used to concentrate and remove actinides from water samples. Tracer was used to monitor chemical

recoveries and correct results to improve precision and accuracy. In this work, 97% chemical recovery achieved.

3. Results and Discussion

The result for samples analyzed is shown in Table 1 and Figure 2. Results for Radium are presented in pCi/L and Bq/L. The highest ^{226}Ra activity concentration (6.7pCi/L) was recorded at Yimirdallang (Figure 2, Table 1 (Y/DALLANG)), some few kilometers southwest of the Zona uranium mineralized area.

Table 1: Radionuclides Levels in Groundwater of the Study Area

S/N	Latitude	Longitude	^{226}Ra	^{226}Ra	^{228}Ra	^{228}Ra	^{232}Th
			(pCi/L)	(Bq/L)	(pCi/L)	(Bq/L)	($\mu\text{g/L}$)
1	10 ⁰ 16'.4	11 ⁰ 45'.6	1.8±0.0486	0.0666	1±0.025	0.037	0.11±0.013
2	10 ⁰ 23'.3	11 ⁰ 50'.6	4.3±0.116	0.1591	2.9±0.073	0.1073	0.08±0.002
3	10021.4	11 ⁰ 58'.2	0.9±0.0243	0.0333	0.3±0.008	0.0111	0.07±0.001
4	10020.4	11 ⁰ 55'.3	0.7±0.0189	0.0259	0.3±0.008	0.0111	0.63±0.012
5	10019.6	11 ⁰ 53'.0	6.7±0.1809	0.2479	4.2±0.105	0.1554	0.04±0.001
6	10 ⁰ 24'.2	11 ⁰ 53'.3	1.5±0.0405	0.0555	1.2±0.03	0.0444	0.05±0.001
7	10 ⁰ 23'.3	11 ⁰ 50'.6	0.6±0.0162	0.0222	0.1±0.003	0.0037	0.02±0.001
8	10 ⁰ 23'.1	11 ⁰ 49'.3	0.3±0.0081	0.0111	<dl		0.03±0.001
9	10 ⁰ 23'.1	11 ⁰ 41'.5	1±0.027	0.037	0.2±0.005	0.0074	0.3±0.006
10	10 ⁰ 26'.4	11 ⁰ 41'.3	1.5±0.0405	0.0555	0.7±0.018	0.0259	0.15±0.003
11	10 ⁰ 22'.1	11 ⁰ 44'.4	2±0.054	0.074	1±0.025	0.037	0.11±0.002
12	10 ⁰ 19'.6	11 ⁰ 46'.2	2.1±0.0567	0.0777	1.6±0.04	0.0592	1.1±0.021
13	10 ⁰ 20'.1	11 ⁰ 47'.3	0.9±0.0243	0.0333	1±0.025	0.037	0.05±0.001
14	10 ⁰ 19'.5	11 ⁰ 45'.4	0.2±0.0054	0.0074	<dl		0.02±0.001
15	10 ⁰ 16'.0	11 ⁰ 40'.5	1±0.027	0.037	0.5±0.013	0.0185	0.22±0.004
16	10 ⁰ 21'.3	11 ⁰ 57'.1	0.9±0.0243	0.0333	0.2±0.005	0.0074	0.31±0.006
17	10 ⁰ 23'.1	11 ⁰ 56'.4	0.7±0.0189	0.0259	<dl		0.07±0.001
18	10 ⁰ 17'.2	11 ⁰ 57'.5	4.2±0.1134	0.1554	3.3±0.083	0.1221	0.04±0.001

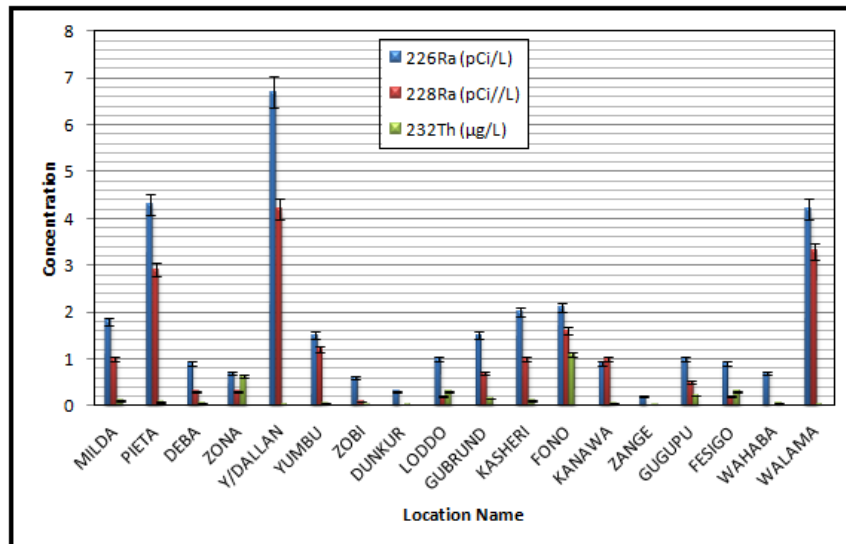


Figure 2: A Graph of Levels of Studied Radionuclide in Groundwater of the Study Area

As can be seen on the map of configuration of water table and groundwater flow direction (Figure 6), the high ²²⁶Ra activity concentration (Figure 3) might have originated from the Zona uranium mineralized area and transported to this area by groundwater as indicated by the flow direction (Figure 6). Analytical protocol specified by the U.S. Environmental Protection Agency (USEPA) in the interim regulations of 1996 recommends that if ²²⁶Ra in drinking water exceed 3pCi/L, then the sample is tested for ²²⁸Ra. Current WHO guidelines have set ²²⁶Ra and ²²⁸Ra maximum contaminant limits at 20pCi/L.

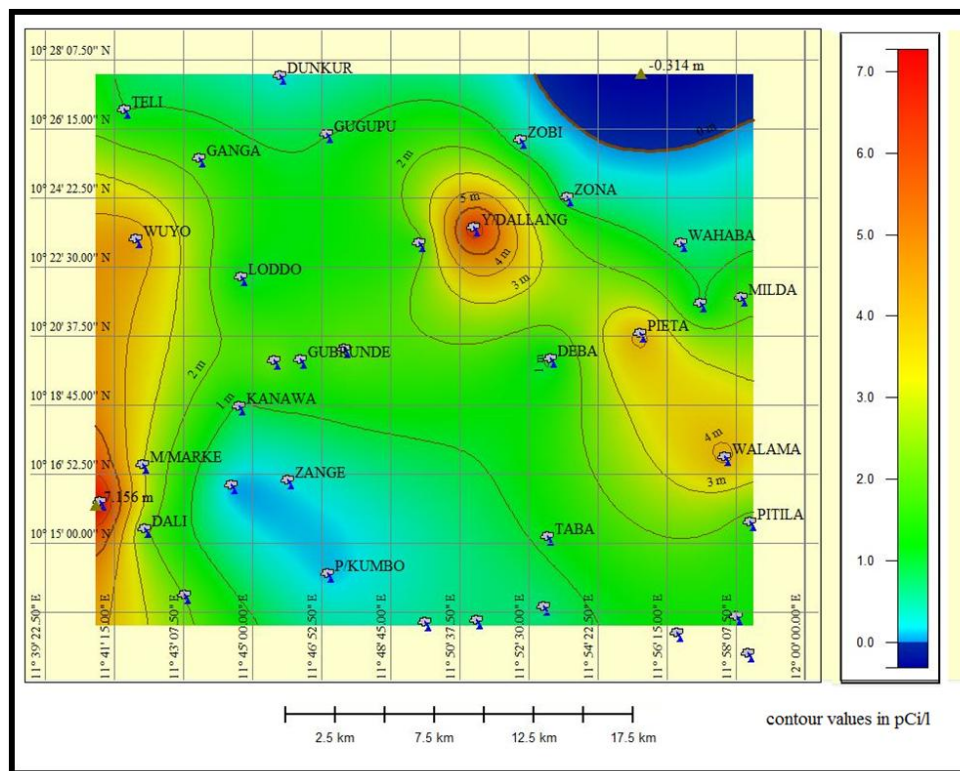


Figure 3: Map of ²²⁶Ra Activity Concentration in Groundwater of the Study Area (Contour Values are in pCi/L)

The setting of separate guideline value for Radium by USEPA was because Radium is believed to be the most radiotoxic of the radionuclides in drinking water (Cothorn, 1987). Of all the samples studied, only two (Pieta and Yimirdallang) had $^{226}\text{Ra} > 3\text{pCi/L}$ (Figure 3) which requires test for ^{228}Ra according to the EPA regulation of 1996.

The activity concentrations of Radium (Figures 3 and 4) in all the studied water samples fall below the EPA's MCL of 20pCi/L for both ^{226}Ra and ^{228}Ra . This means that based on Radium concentration in the studied samples, all the studied water sample are Radium compliant. Thorium levels recorded in the studied groundwater samples ranged from below the detection limit to 1.1 $\mu\text{g/L}$ (Table 1, Figure 5). Thorium is not a regulated contaminant in the WHO, EPA and NIS guidelines and therefore, no health guidelines were proposed for it by these bodies.

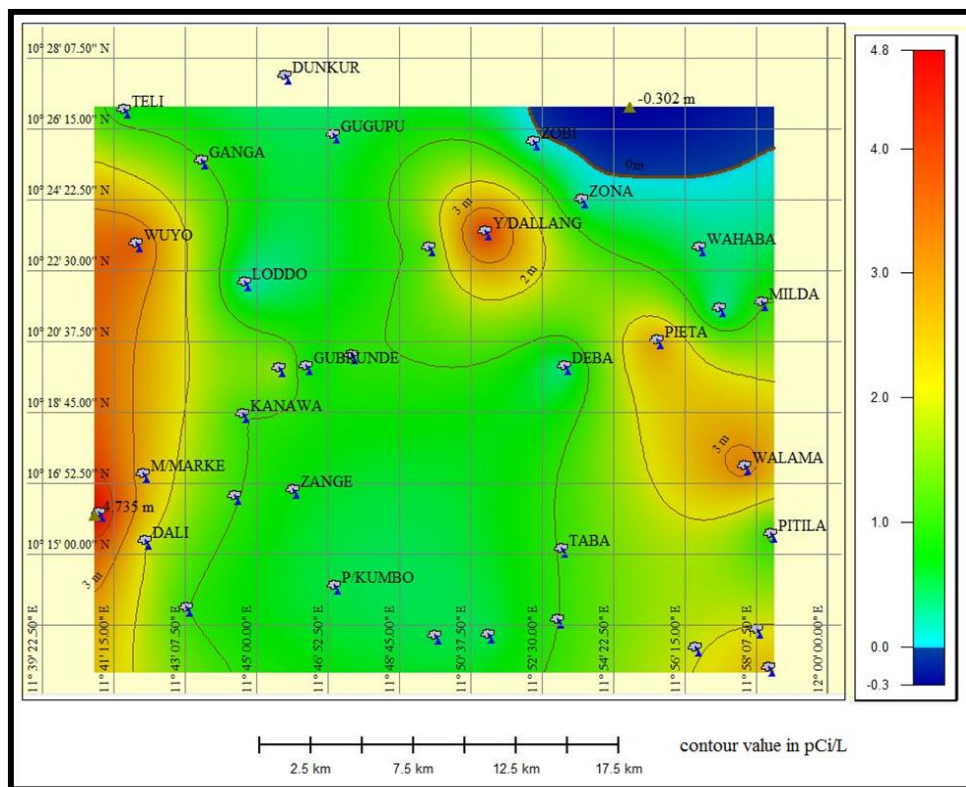


Figure 4: Map of ^{228}Ra Activity Concentration in Groundwater of the Study Area (Contour Values are in pCi/L)

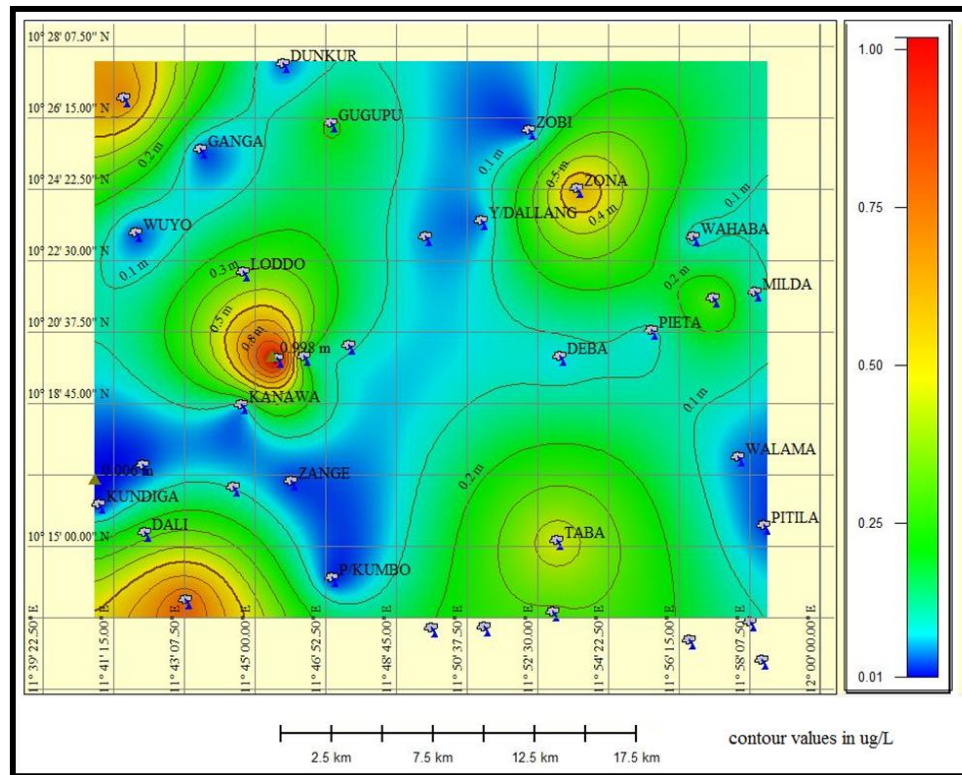


Figure 5: Map of ^{232}Th Concentration in Groundwater of the Study Area (Contour Values are in $\mu\text{g/L}$)

A comparison of Uranium levels in groundwater in the study area (Table 2) and that elsewhere within and outside Nigeria showed that Uranium levels in groundwater from the study area are higher than those from the basement area around Zaria as reported by Onoja (2011).

For Radium, the values from the study area are lower than those reported from other areas in Nigeria by Garba (2010) (Table 2). Awodugba (2008) and Amakum and Jibiri (2010) reported Uranium and Thorium levels in boreholes and wells from southwestern Nigeria to be much higher than those obtained both in this study and from Zaria (Table 2) implying greater effects from ionizing radiation and chemical toxicity after long term consumption of water from those parts of Nigeria.

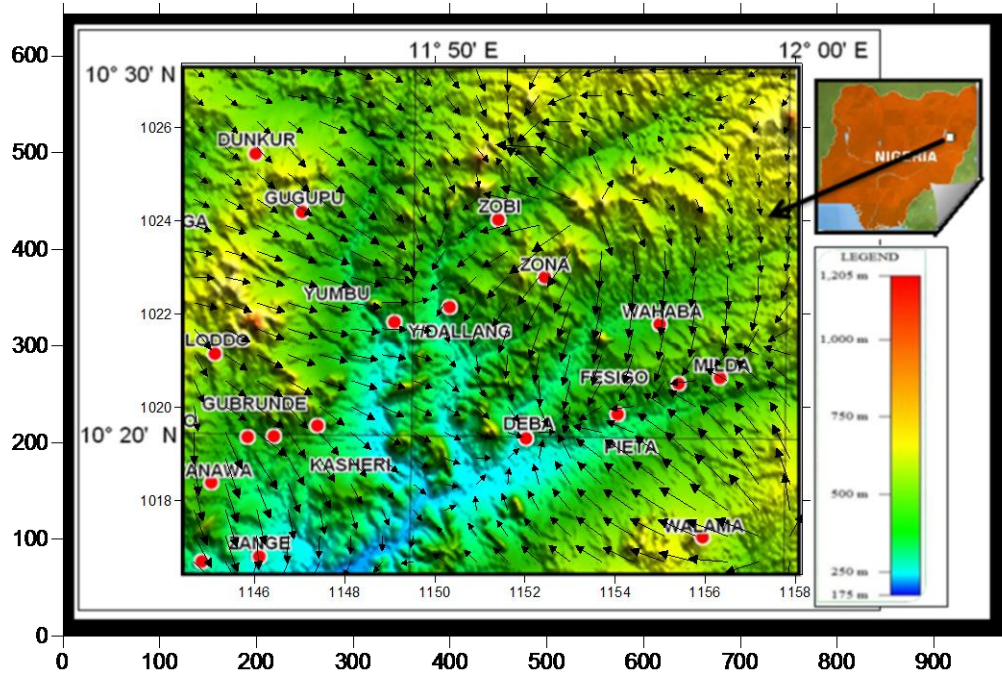


Figure 6: Superimposed Configuration of Water Table with Groundwater Flow Direction on Digital Elevation Model of the Study Area

According to Akerblom and Lindgren (1997), as a result of hydrogeochemical processes occurring in the subsurface, Uranium and its decay products such as Radium may be enriched on the surface of fractures (Figure 7) and based on other previous studies by Gascogne (1997), Langmuir and Riese (1985) and Lingmuir and Melchor (1985), radium appears to be stabilized in solution where high concentration of Ca^{2+} , Mg^{2+} and Cl^- prevails, because these ions compete for adsorption sites.

Table 2: Comparison of U, ^{226}Ra , ^{228}Ra and ^{232}Th Values in Groundwater from the Study Area with Other Reported Value within and outside Nigeria (* are Average Values)

Worker	Radionuclide		
	^{226}Ra (pCi/L)	^{228}Ra (pCi/L)	^{232}Th ($\mu g/L$)
This work (NE, Nigeria)	0.05±0.002 - 7.3±0.19 (*1.87)	0.1±0.003 - 4.8±0.12 (*1.53)	0.01±0.001 - 1.1±0.021 (*0.206)
Garba (2010) (NW, Nigeria)	0.81 - 5.4 (*2.7)	13.5 - 5.14 (*2.43)	
Onoja (2011) (NW, Nigeria)			2.7E5 - 0.00973 (*0.0016)
Amakum and Jibiri(2010) (SW, Nigeria)			
Awodugba (2008) (SW, Nigeria)			297.00±2.58 (*117)

Also, according to Arabi et al. (2012), groundwater from the study area had high Calcium and Magnesium which makes the water very hard; therefore, these might be the reason for Radium stability in groundwater of the area.

Radium itself is not soluble and does not form any soluble complexes that enhance its dissolution into groundwater, but because it is a bone seeker, it is the radionuclides of greatest human-health concern. According to Cothorn (1987), the estimated risk of developing cancer from exposure to total Radium of 5pCi/L is about 10^{-5} .

The most important factor affecting Radium levels in groundwater is the distribution of the parent isotope, and because each Radium isotope comes from separate decay series headed by very different elements, there are very important differences.

The higher levels of ^{226}Ra in the studied samples compared to ^{228}Ra in same sample is as a result of ^{226}Ra being part of ^{238}U decay series. Uranium can be transported in groundwater over long distance and its occurrence can be influenced significantly by secondary process, as a result, ^{226}Ra can be found over a wide range of aquifer types.

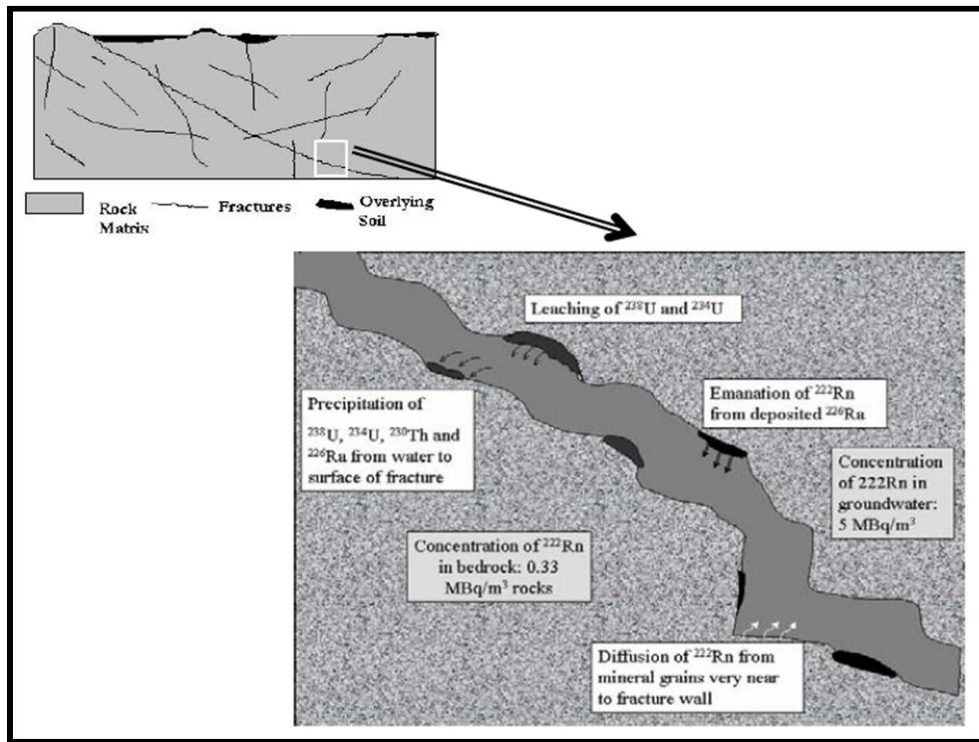


Figure 7: Radionuclides Migration in Crystalline Rocks (Akerblom and Lindgren, 1997)

^{226}Ra is more likely to occur at elevated levels because its parent Uranium can be concentrated into secondary deposits by groundwater. ^{226}Ra is also the third alpha-recoiled progeny in the decay series, making it more susceptible to dissolution. Uranium concentrations above $30\mu\text{g/L}$ has been reported around Yimirdallang and Kundiga (further southwest of the study area) by Arabi et al. 2012, these might have been responsible for substantive ^{226}Ra levels in groundwater of the area while in contrast, ^{228}Ra which is part of the ^{232}Th decay series is lower in sample groundwater samples because Thorium is extremely insoluble and is not subject to mobilization by groundwater. As a result, ^{228}Ra is directly controlled by the distribution of Thorium in the aquifer solids. Where there has been no secondary enrichment of Uranium, ^{228}Ra is generally the dominant Radium isotope in solution, primarily due to the higher natural abundance of Thorium over Uranium.

4. Conclusion

The levels of ^{226}Ra , ^{228}Ra and ^{232}Th in groundwater of the study area indicate the likelihood that Radium distribution in groundwater of the study area might have been controlled by groundwater movement and the distribution of their parent isotopes. Higher ^{226}Ra when compared with ^{228}Ra might be an indication of secondary mineralization of Uranium while low ^{228}Ra levels might indicate the non-solubility of Thorium because an important consequence of the significance in difference in the solubility of the parent isotopes of ^{226}Ra versus ^{228}Ra is that Uranium could be preferentially leached

out of an aquifer, leaving Thorium behind. Consequently the gross alpha and ^{226}Ra would be low. When ^{226}Ra is low it means that ^{228}Ra is even lower and the analysis for ^{228}Ra would not be triggered as recommended by EPA.

Acknowledgement

The authors wish to acknowledge the financial support received from McArthur Foundation, Ahmadu Bello University, Zaria. The Northeast Wale Branch of the International Association of Hydrogeologists (IAH) and GIS Trainings received from Dr. Ewa Kurowska of the University of Silesia in Katowice through sponsorship by the Polish National Commission for UNESCO. Also acknowledged is the financial and logistics support received from management of the Center for Energy Research and Training, Ahmadu Bello University, Zaria, Nigeria.

References

- Akerblom G., et al. *Mapping of Groundwater Radon Potential*. European Geologist. 1997. 5; 13-22.
- Amakum C.M., et al. *Chemical and Radiological Risk Assessment of Uranium in Borehole and Well Water in the Odeda Area, Ogun State, Nigeria*. International Journal of the Physical Sciences. 2010. 5 (7) 1009-1014.
- Arabi A.S., et al. *Activity Concentration of Uranium in Groundwater from Uranium Mineralized Areas And it's Neighborhood*. Journal of Radioanalytical and Nuclear Chemistry. 2012. 293 (1) 135-142.
- Awodugba A.O., et al. *Assessment of Radiological Concentration in Water Supply from Boreholes in Ogbomosho Land, Western Nigeria*. Indoor and Built Environment. 2008. 17 (2) 183-186.
- Cothorn C.R., 1987a: *Development of Regulations for Radionuclides in Drinking Water*. Radon, Radium and Other Radioactivity in Groundwater, Lewis Publishers, Chelsea MI, USA, 1-11.
- Elegba S.B., et al. *Distribution Pattern of REE and Other Elements in the Host Rocks of the Gubrunde Uranium Occurrence, NE Nigeria*. Journal of Radioanalytical and Nuclear Chemistry. 1993. 7; 365-373.
- EPA, 2000: *National Primary Drinking Water Regulations; Radionuclides*. United State Environmental Protection Agency (EPA). Final Rule, 231.
- EPA, 2005: *Human Health Fact Sheet*. Argonne National Laboratory, US, 17.
- EPA, 2010: *The Analysis of Regulated Contaminant Occurrence Data from Public Water Systems in Support of the Second Six-Year Review of National Primary Drinking Water Regulations*. Office of Ground Water and Drinking Water, Washington, DC.
- Funtua, 1985: *An Orientation Biogeochemical Survey on Some Mineral Occurrences in the Peta Syncline, Sheet 153(Wuyo)*. Unpublished B.Sc. Thesis, Ahmadu Bello University, Zaria, Nigeria, 42.
- Funtua, 1988: *Geology and Genesis of Uranium Mineralization at Kanawa, Gubrunde Horst Northeastern Nigeria*. Unpublished M.Sc. Thesis, Ahmadu Bello University, Zaria, Nigeria., 88.
- Funtua, 1992: *Geolgy and Geochemistry of Uranium Mineralization in Mika Northeastern Nigeria*. Unpublished Ph.D. Thesis, Ahamdu Bello University, Zraia, Nigeria, 181.

Funtua, I.I., et al. *Radon Emanation Study of Uranium Ore Samples from N.E. Nigeria*. Applied Radiation and Isotopes. 1997. 46 (6) 867-869.

Garba, 2008: *Natural Radioactivity of Groundwater in the Precambrian Rocks Around Zaria, North-Central Nigeria*. Unpublished Ph.D. Thesis, Department of Geology, Ahmadu Bello University, Nigeria, 218.

Gascogne. High Levels of Uranium and Radium in Groundwater at Canada's underground Research Lab, Lac du Bonnet, Manitoba, Canada, Applied Geochemistry. 1987. 4; 577-591.

Horwitz. *Separation and Preconcentration of Uranium from Acidic Media by Extraction Chromatography*. Analytica Chimica Acta. 1992. 266; 25-37.

Horwitz. *Separation and Preconcentration of Actinides from Acidic Media by Extraction Chromatography*. Analytica Chimica Acta. 1993. 281; 361-372.

Kressin. *Electrodeposition of Plutonium and Americium for High Resolution Alpha Spectrometry*, Analytical Chemistry. 1977. 49; 842-846.

Langmuir D. *The Thermodynamic Properties of Radium*. Geochimica et Cosmochimica Acta. 1985. 49; 1593-1601.

Langmuir D., et al. The Geochemistry of the Ca, Sr, Ba and Ra Sulfates in Some Deep Brines from Palo Duro Basin Texas, Geochimica et Cosmochimica Acta. 1985. 49; 2523-2432.

Maxwell, 1993: High Speed Separations to Measure Impurities in Plutonium-238 Oxide and Trace Radionuclides in Waste, 34th ORNL-DOE Conference on Analytical Chemistry in Energy Technology. Gatlinburg, TN.

Moon D.S., et al. Pre-concentration of Radium Isotopes from Natural Waters using MnO₂ Resin. Applied Radiation and Isotopes. 2003. 59; 225-262.

Nelson, 1992: *Improved Methods for the Analysis of Radioactive Elements in Bioassay and Environmental Samples*. 38th Annual Conference on Bioassay, Analytical and Environmental Radiochemistry. Santa Fe, NM, US.

Okujeni. *Biogeochemical Investigation into Possible Use of Leaf and Bark Samples of Some Savannah Trees in Prospecting Uranium in Upper Benue Trough*. Nig. Jour. Sci Res., 1987. 1; 57-64.

Okujeni C.D. *A Geochemical Orientation Survey for Uranium in the Peta Syncline and Gubrunde Horst, Upper Benue Trough, Nigeria*. Nieria Journal of Scientific Research. 1990. 3; 27-38.

Okujeni C.D. Geochemical and Gamma Spectrometric Analysis of Ores and Host Rocks of the Kanawa Uranium Occurrence in NE, Nigeria. Journal of Radioanalytical and Nuclear Chemistry. 1994. 178 (2) 375-385.

Onoja, 2011: Determination of Natural Radioactivity and Committed Effective Dose Calculation in Borehole Water Supply in Zaria, Nigeria. Unpublished PhD Thesis, Department of Physics, Ahmadu Bello University, Zaria, Nigeria, 190.

Suh C.E. Host Rock Geology and Geochemistry of the Zona Uranium Occurrence, Peta Gulf Syncline (Upper Benue Trough), Northeast Nigeria. Journal of African Earth Sciences. 2000. 31; 619-632.

WHO, 2004: *Guidelines for Drinking Water Quality*, Vol. 1. World Health Organization, Geneva, 1-494.

WHO, 2008: *World Health Organization Guidelines for Drinking Water Quality*. (Third Edition Incorporating the First and Second Addenda) Vol.1. Recommendation, NCW Classifications Washington, 473.

WHO, 2011: *Guidelines for Drinking Water Quality*, (Fourth Edition) WHO Library Cataloguing-in-Publication Data, NLM Classification. Washington, 541.

Vulnerability and Sustainability of Groundwater Resource in India

S.K. Goyal

Department of Physics, RKSD College, Kaithal, Haryana, India

Correspondence should be addressed to S.K. Goyal, sanjay.ktl@gmail.com

Publication Date: 9 September 2013

Article Link: <http://scientific.cloud-journals.com/index.php/IJAESE/article/view/Sci-130>



Copyright © 2013 S.K. Goyal. This is an open access article distributed under the **Creative Commons Attribution License**, which permits unrestricted use, distribution, and reproduction in any medium, provided the original work is properly cited.

Abstract Water is a resource precious for life. The water cycle has significant role in the maintenance of ecosystems. Surface water and groundwater are important components of the hydrological cycle and are interdependent. The supply of water in suitable quality is steadily decreasing and the demand has increased significantly throughout the world. India has been found to be water stressed and is likely to be water scarce by 2050. The present study attempts to review the vulnerability and sustainability of groundwater resource due to its overexploitation dominated by agricultural sector. It has been revealed that groundwater is being consumed by human activities in these parts at a rate faster than replenished by natural processes. In the process, its quality has also deteriorated.

Keywords *Groundwater, Sustainability, Vulnerability, Quality*

1. Introduction

Water has always been perceived as a gift from God as it rained from heavens and provided the earth with the capacity of supporting life. The water cycle has significant role in the maintenance of life and ecosystems. Physical processes of evaporation, condensation, precipitation, infiltration, runoff, and subsurface flow are involved in the movement of water in the hydrologic cycle. In this process, the nature purifies the water and replenishes the land with fresh water. Fresh and clean water is of fundamental importance to the survival, protection and development of human needs, as well as for the conservation of the environment. The total amount of water on earth is estimated to be about 1400 million cubic kilometers which is enough to cover the earth with a layer of 3000 m depth. However, the reserve of fresh water in nature is limited and its spatial distribution is highly uneven. A small proportion of the quantity existing in rivers, lakes and aquifers is effectively available for consumption and other uses.

Surface water and groundwater are important components of the hydrological cycle and are interdependent. These resources fulfill most of the fresh water requirements in the world. Although water is a renewable resource, yet its supply in suitable quality is steadily decreasing. Moreover, the demand has increased significantly throughout the world due to population growth, socio-economic development, technological and climatic changes (Alcamo et al., 2007). During the last century, the

requirements have grown approximately at a rate twice that of population (UN, 2006). It is widely recognized that many countries are entering an era of severe water shortages. By 2050, about two-third of total population of the world is estimated to be living in water scarce areas (Wallace, 2000). India supports more than 16% of the world's population with only 4% of the total fresh water resources (Singh, 2003). The country has been found to be water stressed and is likely to be water scarce by 2050 (Gupta and Deshpande, 2004). The projections of annual demand for water in India are alarming (Table 1).

Table 1: Projected Water Requirements of India in Billion Cubic Meters (BCM)

Use of Water	1990	2000	2010	2025	2050
Domestic	32	42	56	73	102
Irrigation	437	541	688	910	1072
Industry	-	8	12	23	63
Energy	-	2	5	15	130
Others	33	41	52	72	80
Total	502	634	813	1093	1447

Source: Compendium of Agricultural Statistics, 2002, Ministry of Statistics and Programme Implementation, Government of India

2. Groundwater

Groundwater is defined as water occupying all the voids within a geologic stratum. It is a replenishable resource and has several advantages over surface water (Aswathanarayana, 2001). Generally, it has convenient availability near the point of use, a superior quality, and a relatively low cost of development. Precipitation, stream flow, lakes and reservoirs act as principal sources of natural recharge. Other contribution, known as artificial recharge, occurs from excess irrigation, seepage from canals, and special structures installed for the purpose. Natural discharge occurs mostly as flow to the surface from springs and flow into surface-water bodies such as streams, lakes and oceans. Moreover, groundwater near the surface may return directly to the surface by evaporation from the soil and transpiration from the vegetation. Pumping from wells constitutes the major artificial discharge of groundwater (Todd and Mays, 2005).

Worldwide, agriculture accounts for 70% of the total water consumption, compared to 20% for industry and 10% for domestic use. The advent and rapid spread of energized pumping technologies have enabled speedy groundwater development. This has led to emergence of land use and cropping systems dependent on its reliability. In India, groundwater is used to fulfill more than 85% of domestic water supply in rural areas, about 50% of water requirements for urban areas and industries and more than 55% of irrigation water needs. Moreover, groundwater is predominant source of irrigation in drought years (Jain, 2009). Due to production from irrigated land, agriculture contributes around 30% of India's gross domestic product (GDP). Therefore, a large percentage of national GDP is closely dependent on the availability of groundwater. The continuous rise in groundwater use along with increase in intensity of surface-water supply has helped in bringing green revolution in India, particularly in the north-western region.

2.1. Exploitation of Groundwater and Its Sustainability

The groundwater is threatened by over-exploitation as its development has taken place without proper understanding of its occurrence in time and space (CGWB, 2006). An increase in demand has led to higher withdrawal of groundwater. The abstraction exceeding natural replenishment has generated stress in aquifers causing depletion of water table. Since groundwater is a limited resource, the

enormous development of bore-wells threatens aquifers and cases of declining water tables have been widely reported, particularly in densely populated areas (Narain, 1998).

There is a strong relationship between the development and management of groundwater resources because depletion of water tables, groundwater pollution, water logging and salinity are consequences of over-exploitation and intensive agriculture (Prabhakaran et al., 2009). Moreover, climate change also makes a direct impact on groundwater by way of change in recharge. The levels may take months or years to replenish once pumped for irrigation or other uses. Therefore, risks related to groundwater levels are a cause of serious concern (Custodio, 2002). Temporal delay, variability and change in spatial rainfall pattern is of great concern in tropical arid and semi-arid zones, since in these regions, natural vegetation and agricultural ecosystems are highly sensitive to small variations of rainfall (Singh et al., 1992).

The lowering of groundwater levels has resulted in reduction in individual well yield, growth in well population, failure of bore-wells, drying up of dug-wells, increase in power consumption, changes in the direction and velocity of groundwater flow, and ecological damage (Imtiyaz and Rao, 2008). Further, the environmental effects may also cause reduction of porosity, deterioration of water quality, loss of vegetation, land subsidence, inland ingress of saline water in coastal regions etc. (Figure 1.2). The formation of regional depressions of potentiometric levels in several aquifer systems have been observed due to excessive groundwater use (Biswas, 2003).

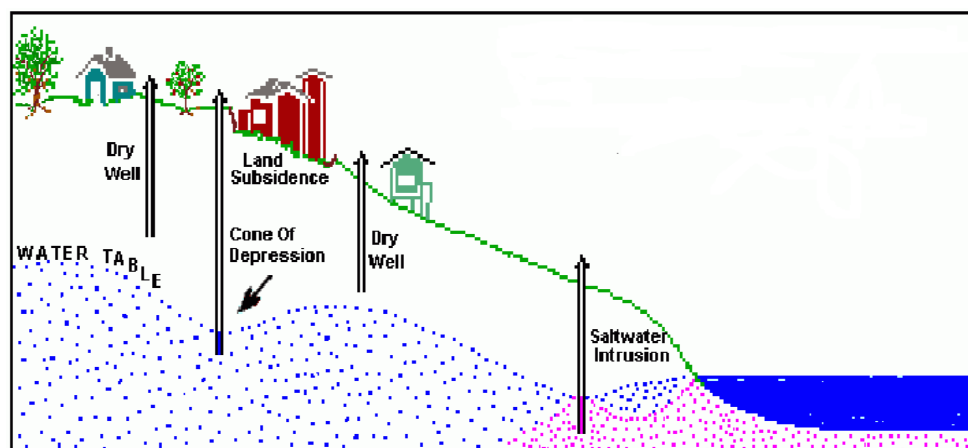


Figure 1.2: Impacts of Overexploitation of Groundwater. Adapted from United States Geological Survey

The factors contributing to unsustainable use of groundwater resources and its degradation in different forms are varied and spatially specific. Excessive withdrawal to meet the needs of increasingly intensive cropping is leading to lowering of water tables in several areas. This is also causing the rise in water table in areas where its use is restricted due to quality considerations, leading to spread of salinity problems. Thus, the problems of unsustainable use of groundwater resources are multifaceted. The optimal use of this resource for a range of diversified and increasing demands requires a good understanding of the issues involved.

2.2. Quality of Groundwater and Its Vulnerability

The quality of groundwater is the resultant of all the processes and reactions that act on the water from the moment it condensed in the atmosphere to the time it is discharged by a well or spring. It varies from place to place and with the depth of the water table (Jain et al., 1995). Due to its unique property of dissolving and carrying in suspension variety of materials with different chemical properties, the groundwater is vulnerable to contamination.

It may acquire minerals and salts from the aquifers during its movement or stay at a location (Todd and Mays, 2005).

Fresh water is essential for domestic, agricultural and industrial uses. The lack of clean drinking water is adversely affecting the general health and life expectancy of the people in many developing countries (Nash and McCall, 1995). Moreover, poor water quality for irrigation is a constant threat to crop yield as well as soil physical conditions (Ayers and Westcot, 1994; Patel et al., 2004; Marechal et al., 2006). Different processes in various industries require huge quantities of water with specific characteristics as water quality may affect their production performances, operational costs and the sustainability. Industrial processes also need good quality water for use as a solvent, a medium, a coolant and a cleansing agent.

Various investigations have shown that groundwater is highly susceptible to pollution from natural as well as anthropogenic factors (Kovar and Krasney, 1995; Appelo and Postma, 1996; Jain and Sharma, 2000). Uncontrolled extraction without commensurate recharge and heavy leaching of pollutants from pesticides and fertilizers to the aquifers has resulted in pollution of groundwater (Rajmohan and Elango, 2005). The changes in direction of groundwater movement due to excessive depletion of water table are causing intrusion of saline water into freshwater zones. Thus, the quality of groundwater has been undergoing a change to an extent that use of such water at certain places could be hazardous for domestic, agricultural and industrial purposes. Moreover, resultant adverse impact on human and livestock population and ecosystem health due to access to toxic elements from agricultural inputs (e.g. fertilizers, pesticides) and industrial effluents is extremely worrisome.

3. The Scenario

In India, a significant decline in the groundwater levels (by more than 20 cm per year) has been observed in 362 districts of the country during the decade 1995-2004 (CGWB, 2006). Moreover, there has been deterioration in groundwater quality due to over-exploitation, indiscriminate use of chemicals in agriculture, and untreated effluents from industrial and domestic sectors (Palaniswami and Ramulu, 1994; Datta et al. 2000). Between 1970 and 1994, the amount of farmland irrigated with groundwater in India increased by 105%, while the areas of land irrigated with surface water increased by only 28%. The rapid increase in groundwater irrigation is also illustrated by the soaring number of mechanized tube wells from less than 10^6 in 1960 to more than 19×10^6 in 2000, making India the country with the maximum number of pump sets (Marechal et al., 2006). Expansion of irrigation led to significant shifts in cropping pattern. Rice followed by wheat emerged as a major cropping sequence. This practice paid off in terms of increased production. But, this has also led to unsustainable use of water resource which has posed a threat to sustaining agriculture and food security of the country.

4. Conclusion

The north-western region of India comprising the states of Punjab, Haryana and western Uttar Pradesh, which was at the centre stage of Green Revolution era during seventies and eighties, now faces serious challenges. It has been revealed that groundwater is being consumed by human activities in these parts at a rate faster than replenished by natural processes. If measures are not taken to ensure sustainable groundwater usage, consequences may include a collapse of agricultural output and severe shortage of potable water for 114 million residents of the region (Rodell et al., 2009).

References

- Alcamo J., et al. *Future Long-Term Changes in Global Water Resources Driven By Socio-Economic and Climatic Changes*. Hydrological Sciences Journal. 2007. 52 (2) 247-275.
- Appelo C.A.J., et al. 1996: *Geochemistry, Groundwater and Pollution*. A.A. Balkema, Rotterdam.1212.
- Aswathanarayana U., 2001: *Water Resources Management and the Environment*. A.A. Balkema, Lisse, the Netherlands.
- Ayers R.S., et al. *Water Quality for Agriculture*. FAO Irrigation and Drainage Paper. 1994. 29 (1) 1–130.
- Biswas S. *Groundwater Flow Direction and Long Term Trend of Water Level of Nadia District, West Bengal: A Statistical Analysis*. Journal of Geological Society of India. 2003. 61; 22-36.
- CGWB, 2006: *Dynamic Ground Water Resources of India*. Central Groundwater Board, Ministry of Water Resources, Govt. of India, New Delhi.
- Custodio E. *Aquifer Over-Exploitation: What Does It Mean?* Hydrogeology Journal. 2002. 10; 254-277.
- Datta S.P., et al. *Effect of Long-Term Application of Sewage Effluents on Organic Carbon, Bio-Available Phosphorus, Potassium and Heavy Metals Status of Soils and Uptake of Heavy Metals by Crops*. Journal of Indian Society of Soil Science. 2000. 48; 836–839.
- Gupta S.K., et al. *Water for India in 2050: First-Order Assessment of Available Options*. Current Science. 2004. 86 (9) 1212-1240.
- Imtiyaz M. et al., 2008: *Influence of Over-Exploitation on Groundwater Ecosystem in Hard Rock Terrain*. Proceedings, International Groundwater Conference, Jaipur, India, 88.
- Jain C.K., et al. *Regression Analysis of Groundwater Quality of Sagar District, Madhya Pradesh*. Indian Journal of Environmental Health. 2000. 42 (4) 159-168.
- Jain C.K., et al. 1995: *Groundwater Quality Monitoring and Evaluation In and Around Kakinada, Andhra Pradesh*. Technical Report, CS (AR) 172, National Institute of Hydrology, Roorkee.
- Jain R.C., et al. *Emerging Challenges for Sustainable Groundwater Management in India*. Journal of Applied Hydrology. 2009. 22 (1) 93–101.
- Kovar K., et al. *Groundwater Quality: Remediation and Protection*. International Association of Hydrological Sciences Publication. 1995. 225; 257-261.
- Marechal J.C., et al. *Combined Estimation of Specific Yield and Natural Recharge in A Semi-Arid Groundwater Basin with Irrigated Agriculture*. Journal of Hydrology. 2006. 329; 281–293.
- Narain V. *Towards a New Groundwater Institution for India*. Water Policy. 1998. 1 (3) 357-363.
- Nash H., 1995: *Groundwater Quality*. In: 17th Special Report. Chapman and Hall, London.
- Palaniswami C., et al. *Effects of Continuous Irrigation with Paper Factory Effluent on Soil Properties*. Journal of Indian Society of Soil Science. 1994. 42; 139–140.

Patel K.P., et al. *Heavy Metal Content of Different Effluents and Their Relative Availability in Soils Irrigated With Effluent Waters Around Major Industrial Cities of Gujarat*. Journal of Indian Society of Soil Science. 2004. 52; 89–94.

Prabhakaran N. *Irrigation Water Quality Status Studies through GIS in Upper Manimukha Sub-Basin, Villupuram District, Vellar basin, Tamil Nadu, India*. Natural Environment and Pollution Technology. 2009. 8 (2) 257-260.

Rajmohan N., et al. *Nutrient Chemistry of Groundwater in an Intensively Irrigated Region of Southern India*. Environmental Geology. 2005. 47; 820–830.

Rodell M., et al. *Satellite-Based Estimates of Groundwater Depletion in India*. Nature. 2009. 460; 789.

Singh A.K., 2003: *Water Resources and Their Availability*. Souvenir, National Symposium on Emerging Trends in Agricultural Physics, Indian Society of Agrophysics, New Delhi; 18-29.

Singh N., et al. *Some Features of the Arid Area Variations over India: 1871-1984*. Pure and Applied Geophysics. 1992. 138 (1) 135-150.

Todd D.K., et al., 2005: *Groundwater Hydrology*. John Wiley and Sons Inc., New York. 3rd Ed. 329–358.

U.N., 2006: *The Millennium Development Goals Report*. United Nations Department of Economic and Social Affairs, New York; 1-32.

Wallace J.S. *Increasing Agricultural Water Use Efficiency To Meet Future Food Production*. Agriculture, Ecosystems & Environment. 2000. 82 (1) 105-119.

WHO, 2006: *Guidelines for Drinking-Water Quality*. World Health Organization, 1: 595.

Impact of Leather and Cosmetic Industries on Quality of Groundwater, in Nagalkeni, Kanchipuram District, Tamilnadu, India

Sridhar S.G.D., Kanagaraj G., Priyalakshmi R., Jobin J., and Baskar K.

Department of Applied Geology and Centre for Environmental Sciences, School of Earth and Atmospheric Sciences, University of Madras, Maraimalai Campus, Guindy, Chennai, Tamilnadu, India

Correspondence should be addressed to Sridhar S.G.D., sgd_sri@yahoo.co.in

Publication Date: 24 September 2013

Article Link: <http://scientific.cloud-journals.com/index.php/IJAESE/article/view/Sci-133>



Copyright © 2013 Sridhar S.G.D., Kanagaraj G., Priyalakshmi R., Jobin J., and Baskar K. This is an open access article distributed under the **Creative Commons Attribution License**, which permits unrestricted use, distribution, and reproduction in any medium, provided the original work is properly cited.

Abstract The area for the present study comprises, Pallavaram, Chromepet, and Nagalkeni, of the Chennai Metropolitan City. Thirty six groundwater samples were collected from open and bore wells during Pre-monsoon (July 2007) and Post-monsoon (January 2008). The parameters like EC, TDS, pH, Ca, Mg, K, Na, SO₄, Cl, and HCO₃ were determined by using standard methods of analysis. The trace elements like, Cu, Cr, Ni, and Pb were determined by using Atomic Absorption Spectrometer. Most of the standard parameters determined in the study area were above the permissible limit. Parameters like sodium, chlorine are found far above the permissible limit, especially in areas near the industrial sites. The type of water that predominates in the study area is (91.7%) Strong acids (Cl) exceed weak acids (HCO₃ and SO₄) during pre-monsoon and (100%) Strong acids (Cl) exceed weak acids (HCO₃ and SO₄) during post-monsoon based on the hydro-chemical facies. The chromium content was far higher than the permissible limit. Leather and cosmetic industries in the study area has deteriorated the quality of groundwater considerably. Thus, this study indicates the impact of effluents from tanneries. The groundwater quality of this region can also be improved by adopting rainwater harvesting thereby increasing groundwater recharge.

Keywords *Leather and Cosmetic Industries, Groundwater, Gibb's Plot, Trace Elements, Piper Diagram*

1. Introduction

Water quality analysis is one of the most important aspects in groundwater studies. The hydro-chemical study reveals quality of water that is suitable for drinking, agriculture and industrial purposes. Further, it is possible to understand the change in quality due to rock water interaction or any type of anthropogenic influence [1, 2]. Globally, groundwater is estimated to provide about 50% of current drinking water supplies. As groundwater is isolated from the surface, most people take it for granted that groundwater be relatively pure and free from pollutants. Although most groundwater is still of high quality, at some locations, it is becoming increasingly difficult to maintain the purity of groundwater [3]. Saline intrusions into coastal groundwater through aquifer penetration have become

a major concern because it is the commonest source of pollution to groundwater [4]. Tanneries are one among those industries which cause high pollution to groundwater as they use a wide range of chemicals, such as sodium chloride, sodium sulphate, chromium sulphate, vegetable oils, lime and dyes. A large quantity of water is also utilized by these industries in the tanning process. Of the 1,200 tanneries in India, Tamil Nadu accounts for more than 75% of these leather processing industries [5]. One of the major problems caused by these industries is high salinity. In addition, there is also a huge quantity of solid waste which results from the hides and skins. Since the solid waste is carelessly disposed, it finds its way into the groundwater during the seasonal rain. It is established that a single tannery can cause the pollution of ground water around a radius of 7 km [6, 7, 8]. This study was carried with the aim of determining the concentration of physical and chemical parameters such as EC, TDS, pH, Ca, Mg, K, Na, SO₄, Cl, HCO₃ and trace elements to assess the present status on quality of groundwater and the impact of Leather and Cosmetic Industries.

2. Study Area and Geology

The study area includes Pallavaram, Chromepet and Nagalkeni areas of the Chennai Metropolitan city. The study area falls between the latitudes from 12°58'02.0" N to 12°57'18.0" N, and longitudes from 80°09'59.9" E to 80°08'02.7" E. The area serves as a hometown for lots of large scale and small scale tanning industries. Chrome tanning is the popular method practiced in this area and hence, the place got its name as chromepet. The study area is 13 km west of the Bay of Bengal. The climate of the area is with low humidity and high temperature. The temperature is around 20°C during winter and reaches a maximum of 44°C during summer. The vegetation in this area is not much varied. The subsurface geology consists of 1 m loamy soil; 2 to 15 m alluvium; 15 to 18 m weathered charnockite and below that there are jointed charnockites for about 20 m and then the bed rock charnockite. The study area with the location of samples is shown in (Figure 1).

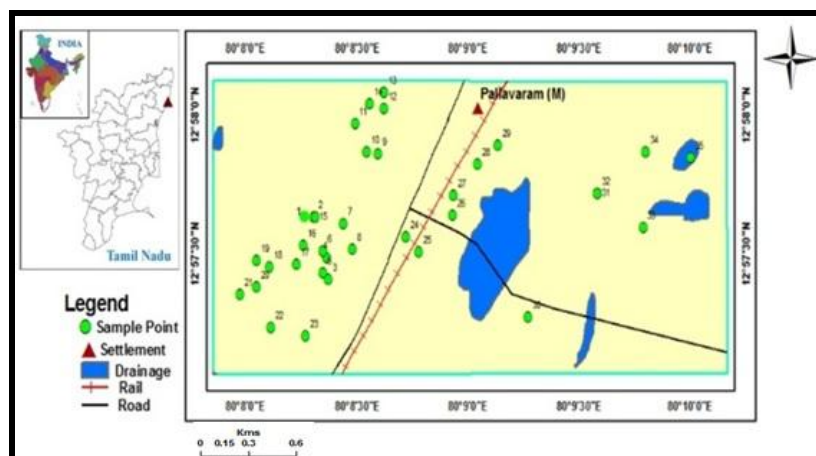


Figure 1: Study Area with Sample Locations

3. Methodology

The water samples were collected from open and boreholes in the study area. One liter of water samples were collected in polyethylene bottles from various wells during the month of July 2007 and January 2008 representing both Pre-monsoon and Post-monsoon. Thirty six groundwater samples were collected for each of the seasons mentioned, for analysis of various physical-chemical parameters. pH were measured using portable pH meter, EC were measured by Electrode in the field itself. Total dissolved solids (TDS) were computed by multiplying the EC by a conversion factor varying from 0.55 to 0.75 depending on the relative concentration of ions [9].

With respect to cation, Calcium, Magnesium was analyzed following volumetric method. Sodium, Potassium was analyzed by Flame photometer; with respect to anions, Chloride, Bicarbonate was done by volumetric method, Sulphate was estimated by turbidity method. Analyses were done following APHA method and the trace elements like, Cu, Cr, Ni, and Pb was determined using Atomic Absorption Spectrometer [10].

4. Results and Discussion

Minimum and Maximum concentration of different parameters and trace elements determined in the groundwater of the study area is presented in Table 1 and Table 2 respectively.

Table 1: Minimum and Maximum Concentration of Different Parameters

Parameters	Pre-monsoon		Post-monsoon	
	Min	Max	Min	Max
EC	200.0	5000.0	1100.0	4800.00
pH	6.1	7.8	5.6	7.90
TDS	128.0	3432.0	704.0	3072.00
Ca	12.0	150.0	20.0	360.00
Mg	1.0	1164.0	2.4	127.20
Na	53.0	1017.0	91.0	1656.00
K	3.0	34.0	1.0	21.00
HCO ₃	54.9	990.6	24.4	104.00
SO ₄	37.9	49.6	28.3	44.04
Cl	124.0	2463.7	26.5	939.42

Table 2: Minimum and Maximum Concentration of Trace Elements

Trace Elements	Pre-monsoon		Post-monsoon	
	Min	Max	Min	Max
Cu	0.244	0.362	0.108	0.307
Cr	0.949	2.725	0.976	1.430
Ni	0.001	0.085	0.009	0.085
Pb	0.038	0.446	0.042	0.598

4.1. Spatial Distribution

A) pH

Groundwater is slightly acidic to alkaline with pH values from 6.5 to 8.3. The pH values of groundwater samples are within the permissible limit [11]. The pH of a solution is the negative logarithm of hydrogen ion concentration in moles per liter. In the pre-monsoon, the pH varies from 6.1 to 7.8 while in the post-monsoon it ranges from 5.6 to 7.9 indicating that the groundwater of the study area is well within the permissible limit. It shows a higher concentration in the northeastern part of the study area during the pre-monsoon season (Figure 2). The highest concentration in the central part during pre-monsoon season may be due to the water bodies that are seen in the study area.

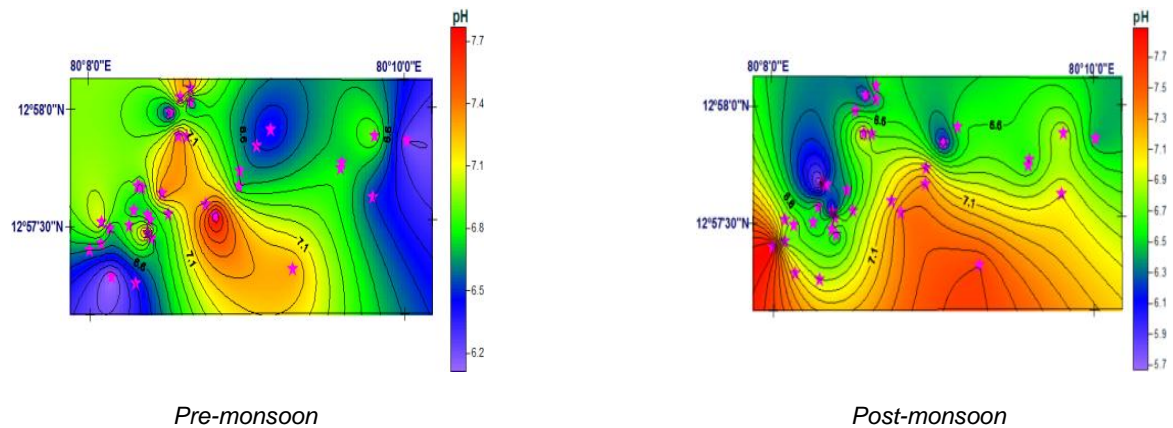


Figure 2: Spatial Distribution of pH Concentration of Pre- and Post-Monsoon

B) Electrical Conductivity (EC) and Total Dissolved Solids (TDS)

Electrical conductivity indicates the capacity of electrical current that passed through the water, which in turn is related to the concentration of ionized substances present in it. Most dissolved inorganic substances present in the water are in ionized form and contribute to electrical conductivity. In the study area, electrical conductivity varies from 200 to 5000 $\mu\text{S}/\text{cm}$ for pre-monsoon water samples, while it ranges between 1100 and 4800 $\mu\text{S}/\text{cm}$ for post-monsoon. Electrical conductivity of water is considered to be an indication of the total dissolved salt content [12]. A rapid estimation of total dissolved solids content in water is obtained by EC. In the pre-monsoon season, the values of TDS are varied from 128 to 3432 mg/l whereas, during the post-monsoon it ranges between 704 and 3076 mg/l. It shows a higher concentration in northern and southern part of the study area during pre-monsoon season (Figure 3).

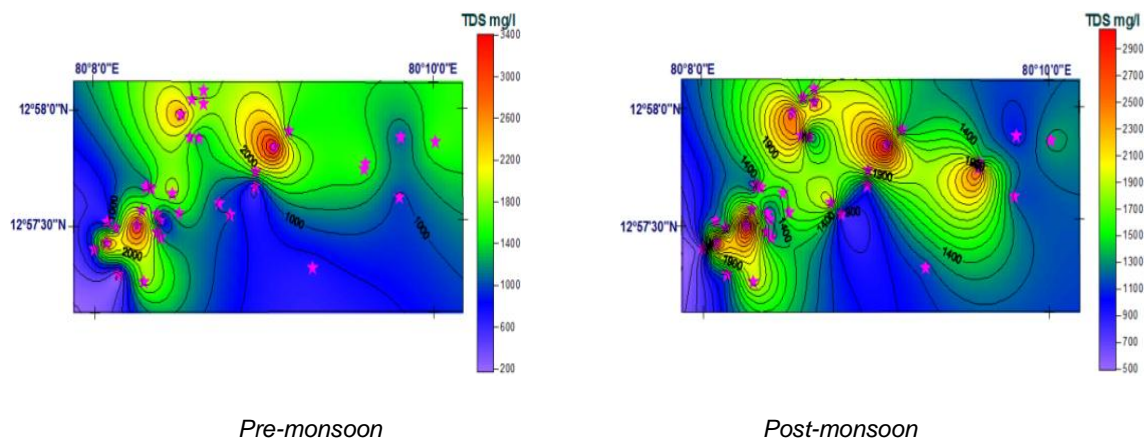


Figure 3: Spatial distribution of TDS concentration of Pre- and Post-Monsoon

C) Cations

Most of the aquifers that contain calcium are dissolved in the groundwater and in that case, the calcium content generally exceeds the magnesium content [13]. Calcium ion concentration in groundwater samples in the pre-monsoon season varies from 12 to 150 mg/l while it ranges between 20 and 360 mg/l during post-monsoon. Magnesium ion concentration in groundwater samples in the pre-monsoon season varies from 1 to 116.1 mg/l while it ranges between 2.4 and 127.2 mg/l during post-monsoon. The concentration of Calcium and Magnesium in the study area may be due to rock weathering. Sodium concentration varies from 53 to 1017 mg/l and from 91 to 1656 mg/l during pre-

and post-monsoon seasons respectively. The concentration of sodium in the groundwater of the study area may be due to rock weathering as well as irrigation return flow.

In general, sodium salts are not actually toxic substances to humans because of the efficiency with which mature kidneys excrete sodium. Higher values of sodium are found in the groundwater in the study area where tanning industries are more compare to other locations. Potassium is slightly less common than sodium in igneous rocks, but more abundant in all the sedimentary rocks. Potassium ion concentration in groundwater samples in the pre-monsoon season varies from 3 to 34 mg/l while it ranges between 1 and 21 mg/l post-monsoon samples.

D) Anion

Chloride concentrations vary widely in natural water and it is directly related to the mineral content of the water. Chloride concentration varies from 124 to 2463 mg/l and from 26.5 to 939.4 mg/l in pre- and post- monsoon seasons respectively. The higher chloride content in groundwater may be attributed to the presence of soluble chloride from rocks and saline water intrusion. Bicarbonate ion concentration varies from 54.9 to 990.6 mg/l and from 24 to 104 mg/l in pre- and post- monsoon seasons respectively. The source for high concentration of bicarbonate may be due to dissolution of CO_3 of the soil and percolation due to irrigation as well as rain water. Sulphate ion concentration varies from 37 to 49 mg/l and from 28 to 44.0 mg/l in pre- and post- monsoon seasons.

E) Piper Diagram

The concentrations of major ionic constituents of groundwater samples were plotted in the Piper trilinear diagram to determine the water type [14]. The classification for the cation and anion facies, in terms of major ion percentages and water types, is according to the domain in which they occur in the diagram segments [15]. The diamond shaped field between the two triangles is used to represent the composition of water with respect to both cations and anions. The points for both the cations and anions are plotted on the appropriate triangle diagrams. The plot of chemical data on diamond shaped trilinear diagram (Figure 4) reveals that the majority of groundwater samples of the study area during both the seasons fall under the facies strong acids exceed weak acids.

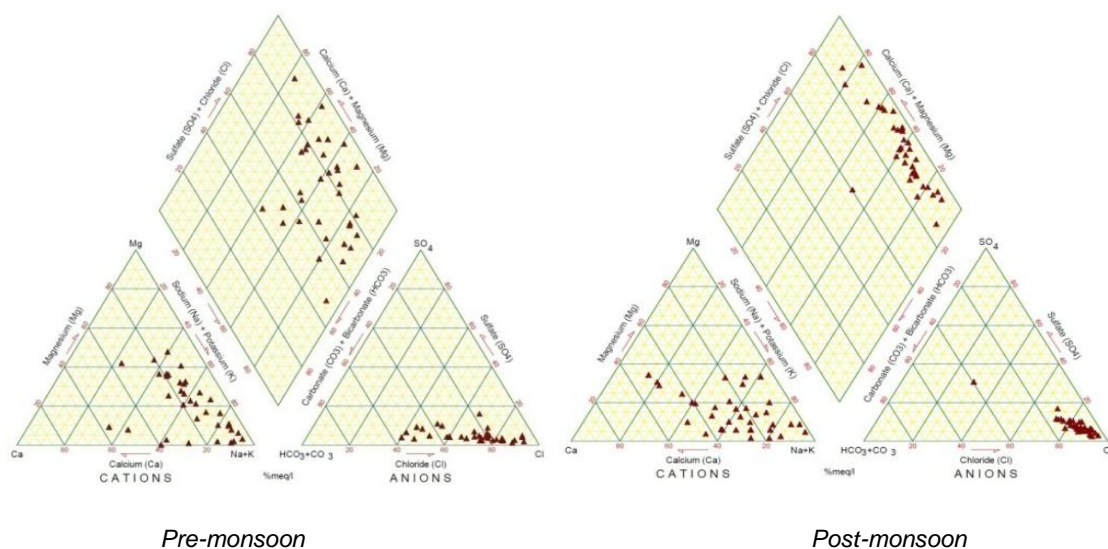


Figure 4: Piper Diagram for Pre- and Post- Monsoon

F) Gibb’s Diagram

Plots of $(Na+K) / (Na+K+Ca)$ versus total dissolved solids (TDS) and $Cl / (Cl+Alk)$ versus TDS (Figure 5) indicate the importance of mineral dissolution [16]. Rengarajan and Balasubramanian; Sreedevi have also used the method to different areas for the evolution of groundwater in various parts of India [17, 18]. Three kinds of fields are recognized in the Gibb’s diagram, namely, precipitation, evaporation, and rock-water interaction. The results show that the anthropogenic activities, like, tanneries present in the study area, are responsible for the chemical composition of the ground water.

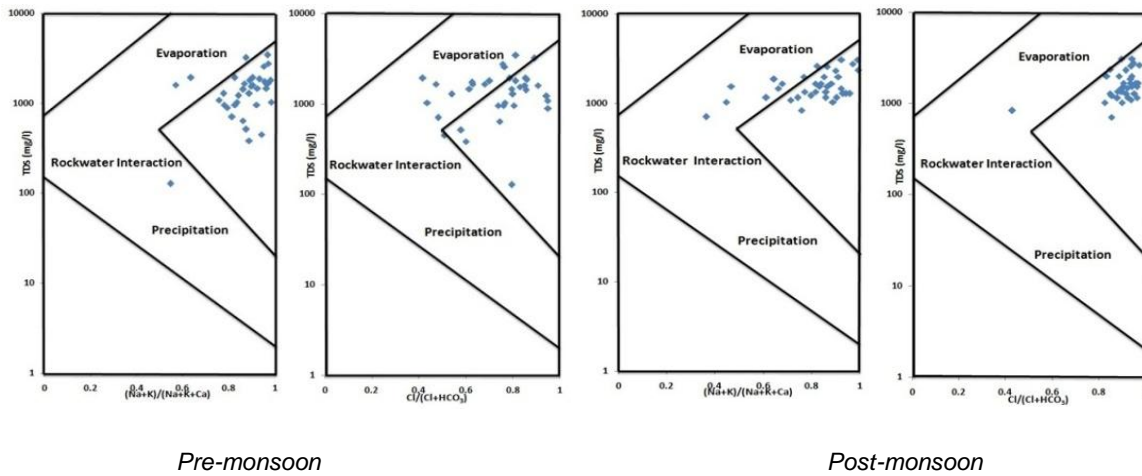


Figure 5: Gibb’s Diagram in Pre and Post Monsoon

G) Chromium and Copper

Tannery effluents are mostly characterized by salinity, high organic loading, and specific pollutants, such as chromium [19, 20]. Chromium which is present in effluents is usually present in the toxic trivalent form. But, when this effluent is discharged into the soil, due to varying environmental conditions, Cr (III) is oxidized to toxic hexavalent form which seldom remains as Cr [21, 22, 23]. Chloride concentration varies from 0.92 to 2.7 mg/l and from 0.97 to 1.43 mg/l in pre- and post-monsoon seasons respectively (Figure 6). Therefore, 95% of the samples are above the permissible limit and thereby creating an awareness to take suitable steps in curtailing the excess chromium concentration in groundwater by properly treating the effluent from tanning industries. Copper concentration varies from 0.24 to 0.36 mg/l and from 0.10 to 0.30 mg/l in pre- and post- monsoon seasons respectively (Figure 7). Copper is required for the synthesis of hemoglobin and several human enzymes whereas in high concentration when consumed, it may lead to neurological complications, like hypertension, liver and kidney problems [24, 25, 26, 27].

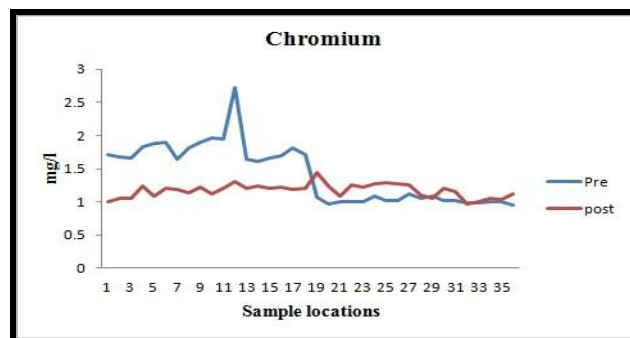


Figure 6: Variation Graph for Chromium during Pre- and Post- Monsoon

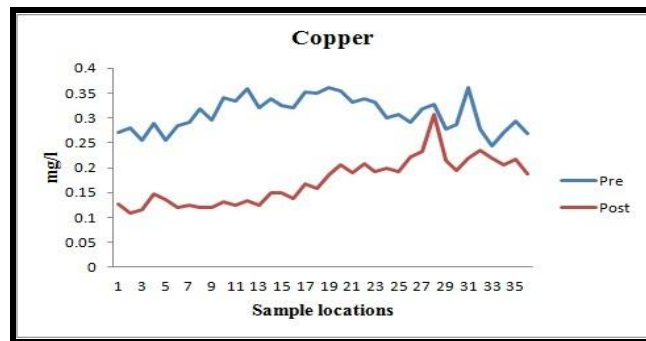


Figure 7: Variation Graph for Copper during Pre- and Post-Monsoon

5. Conclusion

The pH, EC, TDS, parameters analyzed in groundwater during pre-monsoon were relatively lower when compared to post-monsoon. TDS values are indicative of the extent of pollution. The TDS values were seen to increase during the post-monsoon. Ca, Na, Cl, HCO₃, and Mg are showing excessive concentration in some places, in both pre- and post- monsoon periods. The plot of chemical data on the diamond shaped trilinear diagram reveals that majority of groundwater samples of the study area for both the seasons fall under the facies of “Strong acids exceeds weak acids”. The chromium is above the permissible limit in both pre- and post- monsoon. The presence of nickel is below the permissible limit in almost all the samples. High levels of these elements were observed in some groundwater samples collected from sampling wells located very close to tannery industries, which indicates the impact of effluent from the tannery industries which are let onto land and sewerage systems without proper treatment. Artificial recharge and rainwater harvesting can be implemented to improve the present groundwater quality in this area.

Acknowledgement

The authors place on record the financial assistance provided by University Grants Commission, New Delhi under UGC-SAP-DRS I to the Department of Applied Geology, University of Madras for the above said scientific work. Authors thank Prof K.K. Sharma, Professor and Head, Department of Applied Geology and the host institution for according permission and providing facilities to carry out this research program.

References

- [1] Kelley W.P. *Permissible* 1940: *Composition and Concentration of Irrigation Waters*, Proc. ASCE, 66; 607.
- [2] Wilcox L.V., 1948: *The Quality Water for Irrigation Use*. US Dept. Agric., Tech. Bull. 962, Wash., U.S. Dept. Agric. Dc., 40.
- [3] Adewuyi Gregory Olufemi et al. *Assessment of Groundwater Quality and Saline Intrusions in Coastal Aquifers of Lagos Metropolis, Nigeria*. J. Water Resource and Protection. 2010 2; 849-853.
- [4] Batayneh A.T. *Use of Electrical Resistivity Methods for Detecting Subsurface Fresh Saline Water and Delineating their Interfacial Configuration: A Case Study of the Eastern Dead Sea Coastal Aquifers*. Jordan Hydrogeology Journal. 2006.14 (7) 1277-1283.

- [5] Tamilnadu Social Development Report. Tamilnadu Peoples' Forum for Social Development, Chennai, Tamilnadu, India. 2000. 81.
- [6] Bhaskaran T.R., 1977: *Treatment and Disposal of Tannery Effluents*. Central Leather Research Institute (CLRI), Chennai.
- [7] CLRI, 1990: *Report on Capacity Utilization and Scope for Modernization in India Tanning Industry*. Central Leather Research Institute (CLRI), Chennai. 12.
- [8] Ansari A.A., et al. *Status of Anthropogenically Induced Metal Pollution in the Kanpur-Unnao Industrial Region of the Ganga Plain*. Env. Geology. 1999. 38 (1) 25-33.
- [9] Hem J.D., 1991: *Study and Interpretation of the Chemical Characteristics of Natural Water*. U.S. Geological Survey Professional Paper 2254, 3rd Ed. Scientific Publishers, Jodhpur, India, 263.
- [10] APHA, 1998: *Standard Methods for the Examination of Water and Waste Water*. American Public Health Association, Washington.
- [11] WHO, 1984: *Guide Lines for Drinking Water Quality*. Health Criteria and Other Supporting Information Geneva. 2; 973.
- [12] Hem J.D. *Study and Interpretation of the Chemical Characteristics of Natural Water*. USGS Water Supply Paper. 1985. 2254; 117-120.
- [13] CGWB, 2005: *Groundwater Year Book of Andhra Pradesh*. Central Ground Water Board, Ministry of Water Resources, Govt. of India.
- [14] Piper A.M., 1985: *A Graphic Procedure in the Geochemical Interpretation of Water Analyses*. Trans, U.S. Geol. Surv. Groundwater Notes 12, Washington, 42.
- [15] Back W., 1996: *Hydrochemical Facies and Ground-Water Flow Patterns in Northern Part of Atlantic Coastal Plain*. U.S. Geol. Surv. Prof. Paper. 498, 42.
- [16] Gibbs R.J. *Mechanisms Controlling Worlds Water Chemistry*. Science. 1970. 170; 1088–1090.
- [17] Rengarajan et al. *Corrosion and Scale Formation Characteristics of Groundwater in and around Nangavalli, Salem District, Tamil Nadu*. Jour. Appl. Hydrol. 1990. 3 (2) 15-22.
- [18] Sreedevi P.D. *Groundwater Quality of Pageru River Basin, Cuddapah District, Andhra Pradesh*. Jour. Geol. Soc. India. 2004. 64; 619-636.
- [19] Tuney et al. *Use and Minimization of Water in Leather Tanning Processes*. Water Sci. Tech. 1999. 40; 237-244.
- [20] Song Z., et al. *Sedimentation of Tannery Wastewater*. Water Resources. 2000. 34; 2171-2176.
- [21] Anderson R.A. *Chromium as an Essential Nutrient for Humans*. Regul Toxicol Pharmacol. 1997. 26 (1 Pt 2) S35-41.
- [22] Govil P.K., et al. 2004: *Inventorization of Contaminated Sites in India*. NGRI Technical Report No. NGRI-2004-EG-421, 54-66.

- [23] Gowd S.S., et al. *Environmental Risk Assessment and Remediation of Soils Contaminated Due to Waste Disposal from Tannery Industries: A Case Study of Ranipet Industrial Area, Tamilnadu*. *Geochimica et Cosmochimica Acta (GCA)*. 2005. 69 (10) 427.
- [24] Cohen S., 1979: *Environmental and Occupational Exposure to Copper*. In: *Copper in the Environment. Part II, Health Effects*, Ed. Jerome O. Nirayu, John Wiley and Sons, New York, 1-16.
- [25] Larocque et al. *An Overview of Trace Metals in the Environment: Mobilization to Remediation*. *Env. Geology*. 1998. 33; 85-91.
- [26] Rao M.S.R., et al., 2001: *Medical Geology- An Emerging Field in Environmental Science*. National Symposium on Role of Earth Sciences. Integrated and Related Societal Issues, GSI (Geological Survey of India). 65; 213-222.
- [27] Krishna A.K., et al. *Heavy Metal Contamination of Soil around Pali Industrial Area, Rajasthan India*. *Env. Geology*. 2004. 47; 38-44.

Adaptation of RUSLE to Model Erosion Risk in a Watershed with Terrain Heterogeneity

Nadhomi Daniel Luliro¹, John Stephen Tenywa² and Jackson Gilbert Mwanjalolo Majaliwa¹

¹Department of Geography, Geo-Informatics and Climatic Sciences, Makerere University, Kampala, Uganda

²Department of Agricultural Production, Makerere University, Kampala, Uganda

Correspondence should be addressed to Nadhomi Daniel Luliro, danielnadhomi@yahoo.co.uk;
dnadhomi@gmail.com

Publication Date: 28 September 2013

Article Link: <http://scientific.cloud-journals.com/index.php/IJAESE/article/view/Sci-140>



Copyright © 2013 Nadhomi Daniel Luliro, John Stephen Tenywa and Jackson Gilbert Mwanjalolo Majaliwa. This is an open access article distributed under the **Creative Commons Attribution License**, which permits unrestricted use, distribution, and reproduction in any medium, provided the original work is properly cited.

Abstract The modeling capability of the Revised Universal Soil Loss Equation (RUSLE) on a heterogeneous landscape is usually limited due to computational challenges of slope length and slope steepness (*LS*) factor. RUSLE can be adapted to Arc-Macro (C++) executable programs to obtain *LS* values even for highly variable landscapes based on Digital Elevation Models (DEMs); and then predict erosion risk. The objective of this study was to compute *LS* factor from DEM using C++; and predict soil erosion risk in a banana-coffee watershed of the Lake Victoria Basin (LVB) of Uganda. DEM data of Nabajuzi watershed were used as an input file for running the (C++) executable program to obtain *LS* factor. The predicted *LS* values were calibrated against tabulated *LS* values; and a strong linear relationship ($R = 0.998$) was observed between them. The *LS* factor increased with slope length and slope gradient. Erosion risk across landuse were predicted as follows: small scale farmland ($38 \text{ t ha}^{-1}\text{yr}^{-1}$), built up area ($35 \text{ t ha}^{-1}\text{yr}^{-1}$), grassland ($25 \text{ t ha}^{-1}\text{yr}^{-1}$), woodland ($11 \text{ t ha}^{-1}\text{yr}^{-1}$), shrub land and seasonal wetland ($2.5 \text{ t ha}^{-1}\text{yr}^{-1}$), permanent wetland ($0 \text{ t ha}^{-1}\text{yr}^{-1}$). While across soil units erosion risk was highest on Lixic Ferralsols ($50 \text{ t ha}^{-1}\text{yr}^{-1}$), followed by Acric Ferralsols ($20 \text{ t ha}^{-1}\text{yr}^{-1}$), Arenosols ($15 \text{ t ha}^{-1}\text{yr}^{-1}$), Gleyic Arenosols ($2.5 \text{ t ha}^{-1}\text{yr}^{-1}$), and Planosols ($0 \text{ t ha}^{-1}\text{yr}^{-1}$). The risk of erosion increased linearly with slope gradient in the site ($R = 0.96$). On the steepest slopes (15-18) %, the loss ranged from (38–68) $\text{t ha}^{-1}\text{yr}^{-1}$ and on lowest slopes (0-5) %, the loss was (0–2.5) $\text{t ha}^{-1}\text{yr}^{-1}$. We conclude that embedding C++ with GIS data derives *LS* factor from DEMs. It provides a bench mark for understanding slope morphology; hence making erosion risk prediction on non-uniform slopes much easier.

Keywords *Erosion Risk, Slope Length and Steepness, Arc-Macro Language, GIS, Watershed*

1. Introduction

Erosion risk is one of the major threats to sustainable agriculture most especially in the tropics [15]. To foster conservation planning, the USLE and its revised structure (RUSLE) are widely used to model erosion risk to scale [13, 34, 36]. Unfortunately, gross criticisms emerge particularly on the part

of slope length and slope steepness (LS) estimation under non-uniform landscapes. The USLE/RUSLE were typically developed for 9% slope gradient and 22.13 m slope length [43]. It is neither suitable for shorter slopes (less than 4 m) [12], nor for longer ones (greater than 120 m) [33]. Whereas several algorithms have been developed to cater for this purpose, none of them is universally acceptable for LS estimation due spatial terrain heterogeneity. There is paucity of information concerning how spatial heterogeneity at watershed scale affects soil erosion processes to foster its monitoring and conservation planning strategies [35]. By and large, the commonest algorithms used in LS estimation include: the grid-based [18]; unit stream power theory [31, 28, 29]; contributing area [6, 7]; neighborhood and quadratic surface, maximum slope and maximum downhill slope [38].

Many of these algorithms, however, are premised on equations such as Equation 1, which assume the exponents to have constant values. Yet, the most realistic approaches for LS computation are those that are anchored on exponential variability with respect to slope gradient [10, 47].

$$LS = [A/22.13]^m \times [\sin \theta/0.0896]^n \quad (\text{Equation 1})$$

Where m and n have constant values of 0.6 and 1.3, respectively; θ is the terrain slope in degrees; A is the upslope contributing area per unit width of cell spacing ($\text{m}^2 \text{m}^{-1}$) from which the water flows into a given grid cell. According to [29], a derived as the sum of all grid cells from which the water flows into the cell expressed as:

$$A = \frac{n\mu a}{b}$$

where a is the area of the grid cell; n is the number of cells draining into the cell; μ is the weight depending on runoff generation mechanism and infiltration rates; and b is the cell spacing.

Adapting RUSLE to a C++ program circumvents LS estimation loopholes [41], hence boosting its modeling capability under terrain heterogeneity conditions. It is postulated that since water flows down slope under gravity, its flow direction can then be North, South, East or West; or Northeast, Southeast, Southwest or Northwest. This method further assumes that if flow converges occur, then the flow direction would be the side of the steepest descent. Considering the pixel grid in the DEM, the C++ program is able to calculate Non-cumulative slope length (NCSL). NCSL is the distance between the centres of the grid cells of the DEM. A cumulative slope length is then computed by summing the NCSL from each grid cell, beginning at a high point and moving down along the direction of steepest descent. This expeditiously computes the LS factor for use in RUSLE from DEMs under conditions that were highlighted by [17] as follows:

- a. If the cell being calculated is a high point then NCSL = 0.5 (cell resolution size);
- b. If the input cell's flow direction is in a cardinal (N,S,E,W) direction then NCSL = (cell resolution size);
- c. Otherwise (flow is in diagonal direction: NE, NW, SE, SW) and NCSL = 1.4142 (cell resolution size).

The objective of this study was to compute the LS factor from DEM based on C++ script; and to predict soil erosion risk in order to identify hot spots for effective conservation planning in a banana-coffee dominated watershed of the Lake Victoria Basin of Uganda.

2. Materials and Methods

2.1. Site Description

The study site was Nabajuzi watershed of the Lake Victoria Basin (LVB) of Uganda, delineated using a hydrological mapping tool (AvSWAT) (Figure 1). This site covers approximately 939 Km². It is traversed by a swampy-bogged stream draining into the River Katonga system that flows into Lake Victoria. The elevation, 1200-1290 m above sea level, of this area is in part attributed to the geologic disturbances that incurred on the old basement complex rocks of the East African plateau. This watershed rests on the old Buganda surface, which is characterized by hills and ridges that were dissected by streams and water ways [16]. From the data gathered from National Agriculture Research Laboratories (NARL) in Kawanda, Uganda, five soil types classified according to the FAO system exist in the site. These soils include: *Acric Ferralsols* (299.49 km²), *Gleyic Arenosols* (147.74 Km²), *Lixic Ferralsols* (463.78 Km²), *Arenosols* (27.72 Km²) and *Planosols* (0.21 Km²). They belong to Buganda, Mirambi, Mawogola and Kabira catenas; and Mulembo, Kifu and Sango series, respectively (Table 1).

Table 1: Soil Classification and Distribution in Nabajuzi Watershed in the Lake Victoria Basin of Uganda

Area (km ²)	Percent (%)	Parent Rock	Mapping Unit	Classification (FAO)	Productivity
230.0	24.5	Toro gneisses and granites	Mawogola catena	Acric ferralsols	Medium to low
44.3	4.7	Recent alluvium	Mulembo series	Gleyic arenosols	Nil to low
178.8	19.0	Toro gneisses and granites	Mirambi catena	Acric ferralsols	High
27.7	3.0	Basement complex gneisses and granites	Katera series	Arenosols	Medium
463.8	49.4	Toro schists and phyllites	Buganda catena	Lixic ferralsols	High
0.21	0.02	Lake deposits	Sango series	Planosols	Nil to low
103.5	11.0	Alluvium and hillwash from basement complex	Kifu series	Gleyic arenosols	Nil to low
Total = 939		100%			

Source: National Agriculture Research Laboratories, Kawanda, Uganda

2.2. Parameterization of RUSLE Factors to Predict Soil Erosion Risk

Erosion modeling was performed based on RUSLE framework [33] as in Equation (2).

$$A = LS^* R^* K^*C^*P \quad (\text{Equation 2})$$

Where, A = Soil loss in t ha⁻¹ over a period selected for R, usually on a yearly basis;

R = Rainfall-runoff erosivity factor in MJ mm ha⁻¹ hr⁻¹yr⁻¹;

K = Soil erodibility factor in t h MJ⁻¹ mm;

L = Slope length factor (dimensionless);

S = Slope steepness factor (dimensionless);

C = Cover and management factor (dimensionless); and

P = Conservation support practices factor (dimensionless).

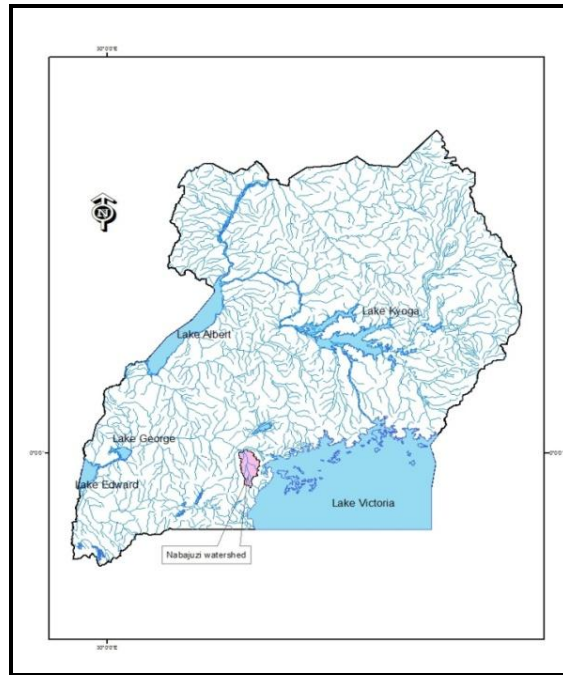


Figure 1: The Drainage Map of Uganda Showing the Location of Nabajuzi Watershed in the LVB

2.3. Procedure for Slope Length and Steepness (*LS*) Estimation

The Arc-Macro Language (AML) method for *LS* calculation was used. It operates in an automatic program, and computes the *LS* values from a DEM to form a single raster layer [41]. This method was first written in an AML [17], but was later updated with the C++ Programming Language to improve its efficiency in data processing. The original AML procedure was hinged on equations that were earlier on developed by [43] for computing slope steepness as:

$$S = (65.41 \times \sin 2\theta) + (4.56 \times \sin \theta) + 0.065 \quad (\text{Equation 3})$$

Where, θ is slope angle in degrees.

However, the upgraded C++ program uses modified slope steepness equations [27] adapted from equation (3) to enable it cater for all terrain variations that could be available in any given watershed. These expressions are presented as in Equation (4).

$$S = 10.8 \times \sin \theta + 0.03, \text{ for slope percent} < 9\%; \text{ and}$$

$$S = 16.8 \times \sin \theta - 0.50, \text{ for slope percent} \geq 9\% \quad (\text{Equation 4})$$

















Where θ is slope angle in degrees.

2.4. Computation of *LS* Factor by Adapting RUSLE to C++ Program

The C++ Programming Language was embedded in an ESRI ArcGIS 9.3 environment. A detailed contour map covering the entire watershed was obtained from Ministry of Lands, Housing and Urban Development, Department of Surveys and Mapping, Entebbe, Uganda. A DEM (coded *nabj*) was created by interpolation from Spatial Analysis Tools. This DEM (30 m by 30 m) resolution was used as an input raster file in the C++ Program. Prior to execution, the DEM was first converted to ASCII format using Raster Conversion Tools for easy recognition by the program. After conversion, the C++

executable program was used to run it. In tandem, a series of commands appeared in the command lines in which the path and filename with DEM data (in ASCII format) were entered. The path for the output files was then appropriately defined to enable easy retrieval. The pixel cells with no data in the DEM were ignored in the computation to improve accuracy and precision. Automatically the program filled any depressions or sinks found on the DEM so that the highest elevation points were easily identified. Flow direction was determined by the program; hence enabling the *LS* factor calculation. After execution, sixteen files with suffix (.dat) each containing a different theme (Table 2) were produced. Only *nabjrusle_l.dat*, *nabjrusle_s.dat* and *nabjrusle2.dat* were used because they contained data required for the *LS* factor. The other files such as: *nabjoutflow.dat* and *nabjslp_cut.dat* contained data for the potential deposition areas in this watershed; while *nabslp_exp.dat* contained slope exponents, but this was beyond the scope of this study.

Table 2: A Display of the C++ Program Files after Executing the DEM of Nabajuzi Watershed of LVB of Uganda

					
nabjcell_len.dat	nabjdemfill.dat	nabjinflow.dat	nabjinit_len.dat	nabjlogfile.dat	nabjorig_dem.dat
					
nabjoutflow.dat	nabjrusle_l.dat	nabjrusle_s.dat	nabjrusle2.dat	nabjslp_ang.dat	nabjslp_cut.dat
					
nabjslp_exp.dat	nabjslp_fac.dat	nabjslp_in_ft.dat	nabjslp_len.dat		

The identified *LS* factor files were then converted back to a raster format by adding the suffix (.txt) using the Conversion Tools function in ArcGIS 9.3. The new raster files *nabjrusle_l.txt*; *nabjrusle_s.txt* and *nabjrusle2.txt* were all imported as one layer to form an *LS* factor map of Nabajuzi watershed.

2.5. Procedure for Rainfall Erosivity (*r*) Factor Estimation

The rainfall erosivity factor (*R factor*) is defined as the average annual total of the storm *EI*₃₀ values for a place [33]. *EI*₃₀ is the individual storm index values which equals to *E*, which is the total kinetic energy of a storm, multiplied by *I*₃₀ which is the maximum rainfall intensity in 30 minutes. The multiplication of *EI* reflects the total energy and peak intensity combined in each particular storm. Continuous rainfall records are necessary to calculate the maximum 30 minute rainfall intensity (*EI*₃₀). To obtain an accurate *R factor*, *EI*₃₀ needs to be calculated with continuous records over multiple years for multiple stations located at the area of the study site. The basic equation for determining the *R factor* was earlier developed by [42] as presented in Equation (5).

$$R = \frac{1}{n} * \sum_{j=1}^n [\sum_{k=1}^m (E) * (I_{30})] \quad \text{(Equation 5)}$$

Where: R = Rainfall erosivity factor;

E = Total storm kinetic energy (MJ/ha);

*I*₃₀ = Maximum 30 minute rainfall intensity;

j = Index representing the number of years used to compute the average;

k= Index representing the number of storms in each year;
 n = Number of years to obtain the average; and
 m = Number of storms in each year.

Since total energy (E) and maximum 30-minute intensity (I_{30}) are the rainfall characteristics that are most closely related to the amount of soil erosion produced in an area, the EI_{30} values can be calculated for each rainfall that exceeds 13mm. For this reason, some authors have argued that kinetic energy (E) can be determined from the Equation (6), which was developed by [9].

$$E = 118.9 + 87.3 \log I \quad (\text{Equation 6})$$

Where: E = kinetic energy ($\text{J m}^{-2} \text{mm}^{-1}$); and I = rainfall intensity (mm hr^{-1}).

Alternatively, a modified Fournier index can also be used to estimate the R -factor as used by [20]. Basing on this method, average annual EI_{30} is expressed in $\text{MJ ha}^{-1} \text{mm}^{-1} \text{hr}^{-1}$ is calculated from Equation (7).

$$EI_{30} = 0.3 * \sum(p_i/P)^{1.93} \quad (\text{Equation 7})$$

Where: p_i = mean monthly rainfall (mm); and P = mean annual rainfall (mm).

But criticism has enthralled this index based on the fact that even light rains can cause significant erosion depending on other factors such as soil properties; slope length, steepness, antecedent moisture and vegetation cover [1].

In Vietnam, [14] pointed out that rainfall erosivity indices could simply be determined from mean annual totals as shown in the Equation (8).

$$R = 0.548P - 59.9 \quad (\text{Equation 8})$$

Where: R = rainfall erosivity (J m^{-2}); and P = mean annual rainfall of the area (mm).

While in Indonesia, an earlier study by [3] recommended the use of Equation (9) to determine the rainfall erosivity factor for erosion studies.

$$R = 2.5 * P^2 / [100(0.078P + 0.78)] \quad (\text{Equation 9})$$

Where: R = rainfall erosivity (J m^{-2}); and P = annual rainfall (mm).

In East Africa, standard erosivity indices are usually determined from Equation (10) which was developed by [30].

$$R = 0.029 (3.96P + 3122) - 26 \quad (\text{Equation 10})$$

Where: R = rainfall erosivity (J m^{-2}); and P = the mean annual rainfall of the area (mm).

This index is robust in the sense that it recognizes and computes the erosivity of rainstorms with varying intensities, a salient feature of the torrential rains received in this region. For this reason, this index has been accepted and widely used in different agro-ecological zones of Uganda to estimate rainfall erosivity [24, 25, 2].

2.6. Determining Soil Erodibility (*K*) Factor

Two methods were employed to derive the soil erodibility *K* factor. First, was obtaining soil samples from all the soil units in the site; and establishing the soil erodibility values by nomograph method [43, 33]. This method uses percent silt plus very fine sand (0.002-0.1 mm), percent sand (0.1-2 mm), percent organic matter, and soil structure and permeability classes to calculate the *K* values. Soil structure was interpreted from soil profile descriptions that were made for each soil unit in the site; while permeability codes were assigned to each horizon. Second, was by using the soil layer obtained from National Agricultural Research Laboratories, Kawanda (KARL) and adding soil erodibility values for each soil unit to its attribute table. These erodibility values were computed from the basic Equation (11), which was developed by [43].

$$100K = 2.1M^{1.14}10^{-4}(12 - a) + 3.25(b - 2) + 2.5(c - 3) \quad (\text{Equation 11})$$

Where, *M* = topsoil texture, calculated as (%silt + % silty sand)*(100% - % clay);
a = % of topsoil organic matter content;
b = class of topsoil structure; and
c = class of soil profile permeability.

The corresponding *K* values obtained for each soil unit were added to the table of attributes using the Add Field function in ArcGIS 9.3 to the soil map. This map was then used to generate an erodibility map for the study site.

2.7. Determination of the Crop Cover and Management (*C*) Factor

The *C* factor reflects the effect of cropping and management practices on erosion rates. The *C*-factor could be extracted by an algorithm which combines landuse, canopy cover, surface cover, surface roughness and soil moisture as sub-factors [33]. But some of these parameters may not readily be available for some areas. Thus, circumventing this pitfall, [36] recommended the use of percent canopy- or surface-cover alone to estimate this factor as shown in Equation 12, a method which was adopted for use in the study site in conjunction with image processing.

$$C = 0.6508 - 0.343\log c; \text{ for } 0 < c < 78.3\% \quad (\text{Equation 12})$$

Where: *C* equals 1 and 0, if *c* is equal to 0% and $\geq 78.3\%$, respectively; and *c* is percentage canopy/surface cover.

To generate the *C* factor map, a Landsat Enhanced Thematic Mapper (30 m by 30 m) image of 2010 was acquired and processed using procedures described by [22]. A linear image enhancement technique was performed to increase contrast of features in this image. A pseudo color composite was made with bands 4, 3 and 2, for easy identification of the various land use and land cover types in the watershed. This image was classified using supervised classification procedure using Erdas imagine 9.2. A preliminary land use and cover map was then obtained using the maximum likelihood classifier algorithm. Coupled to this, ground truthing was conducted on-site to synchronize particular land use and cover categories with image classes and the National Biomass data for 2006 (classified according to FAO System), which were obtained from National Forestry Authority (NFA), Nakawa. The *C* factor layer was finally obtained by adding the computed *C* values to the attribute table of the landuse map. These values were obtained based on percent bio-mass for each landuse and land cover class.

2.8. Deriving the Conservation Practice P Factor

No erosion physical control structures were identified in the site. The conservation practice factor, P was therefore regarded as 1. The layer for this factor was created by re-classifying the DEM image of this watershed. A value 1 was assigned to replace the elevation values for each of DEM grid cells using Spatial Analyst tools, and by selecting the Re-classify Function. The range of values was reset under the column 'old values' from the lowest to highest elevation values of the DEM to make all values of its cells correspond to 1, hence giving rise to a new class which now constitute the P factor layer.

3. Results and Discussion

3.1. Calibration of the LS Values of Nabajuzi Watershed

The predicted LS values obtained from the executed DEM of Nabajuzi watershed using the C++ program was calibrated against tabulated LS values for moderate ratio of rill to interrill erosion generated Technical Guide to RUSLE use in Michigan, NRCS-USDA State Office of Michigan [32]. The predicted and tabulated LS values were correlated; depicting a strong ($R = 0.998$) linear relationship between them as presented in Figure 2. For shorter slope lengths with low gradients, the predicted and tabulated LS values generally conformed to each other. In addition to this, a close association of the said values was also recognized in situations where longer slopes existed at low slope angles. By and large, the predicted LS values were utilized as authentic values for use in erosion prediction in Nabajuzi watershed due to the strength of their correction with the tabulated values for rill and interrill erosion.

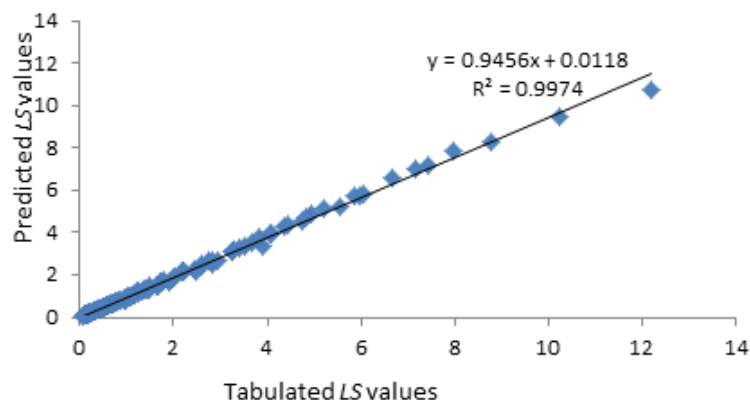


Figure 2: Correlation between the Predicted and Tabulated LS Values for Nabajuzi Watershed of Uganda

3.2. Erosion Risk Spots in Nabajuzi Watershed

Figure 3 shows the spatial patterns of soil erosion risk in Nabajuzi watershed. Soil erosion risk ranged from 0 to 125 t ha⁻¹yr⁻¹. These extreme cases were predicted in the valleys and in areas with bare soil or steep slope gradients, respectively. Soil erosion was described as nil (0 t ha⁻¹yr⁻¹), very low (1-5 t ha⁻¹yr⁻¹), low (6-10 t ha⁻¹yr⁻¹), moderate (11-20 t ha⁻¹yr⁻¹), high (21-40 t ha⁻¹yr⁻¹), and very high (41-125 t ha⁻¹yr⁻¹). With respect to the spatial pattern of erosion severity, all areas with high to very high erosion magnitude were considered as soil erosion hotspots in this watershed.

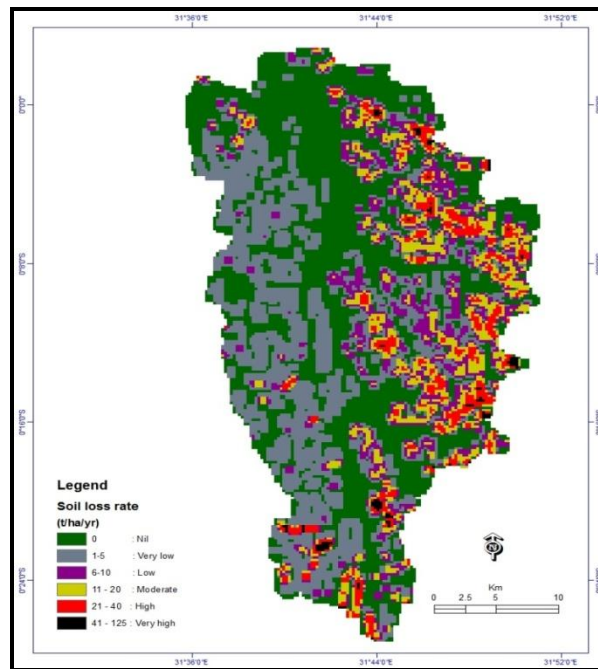


Figure 3: Spatial Pattern of Soil Erosion Risk in Nabajuzi Watershed in the LVB of Uganda

3.3. Variation of Erosion Risk with Landuse

The risk potential predicted for the different landuse is presented in Figure 4. This potential was highest in small scale farmland ($38 \text{ t ha}^{-1}\text{yr}^{-1}$), followed by built up area ($35 \text{ t ha}^{-1}\text{yr}^{-1}$), grassland ($24 \text{ t ha}^{-1}\text{yr}^{-1}$), woodland ($11 \text{ t ha}^{-1}\text{yr}^{-1}$), shrub land and seasonal wetland ($2.5 \text{ t ha}^{-1}\text{yr}^{-1}$) and lowest in permanent wetland ($0 \text{ t ha}^{-1}\text{yr}^{-1}$).

The high soil erosion risk potential in small scale farmland was expected as tillage destroys soil structure, making the soil highly susceptible to raindrop impact and runoff. This contradicts earlier findings by [8] and [21] who contended that a farmland can have less soil loss under proper management conditions. With regard to the Nabajuzi watershed, a common feature is that little ground cover management (mulches) coupled with the lack of physical structures for erosion control were originally identified as some of the most important concerns that underlain the high soil loss rates on cultivable land [40, 24].

The predicted soil erosion risk in the grassland, woodland, shrub land, seasonal and permanent wetlands were also expected and seemed to conform to the idea raised by [37] about the impact of vegetation in reducing runoff and soil loss. As canopy reduces raindrop impact, trees themselves also provide litter on the soil surface which decomposes to yield soil organic matter (SOM). This condition warrants soil aggregate stability towards runoff [26]; hence, generating moderately low erosion rates in these landuse as indicated in Figure 4. Besides, the roots bind the soil particles, increase macro pores in the soil, enhancing water infiltration, transpiring soil water and providing additional surface roughness by adding organic substances to the soil [39]. Plenty of literature indicates that grass cover is the most effective in reducing water erosion as compared to forest cover [4, 48, 5]. An unusual situation was recognized in the site whereby the grassland had more soil lost due to runoff as compared to the woodland area. A common practice is that in this watershed the grassland is usually degraded either through bush burning to regenerate pastures for animal grazing; or through cutting grasses to obtain residues for use as mulches in farms. This situation increases soil erosion particularly in the said landuse. On the other hand, the woodland in this site may have had a low soil loss rate compared to the grassland partly due to above ground cover as already discussed; or due to the root mechanical effect on soil strength as was previously claimed by [44]. The built up area had a

high soil loss rate because of existence of exposed soil surface in some parts, in addition to existence of concretized surfaces and roofs which increase the volume of runoff hence increasing soil loss most especially in the nearby highly susceptible soils.

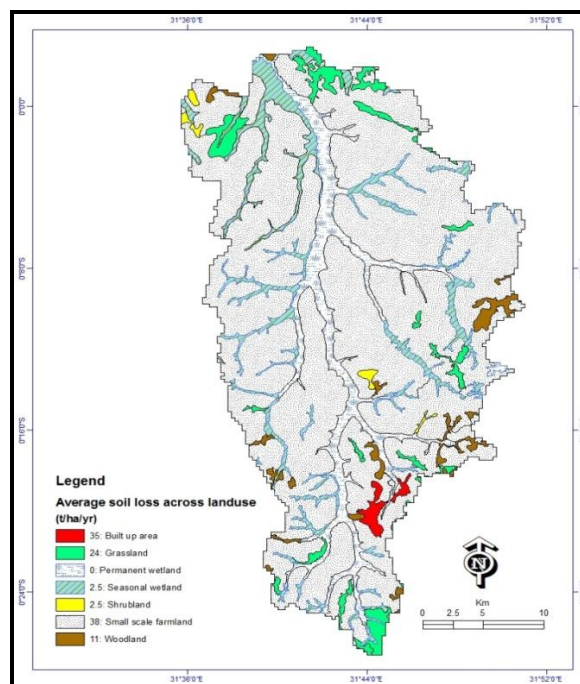


Figure 4: Variation of Soil Loss with Landuse Category in Nabajuzi Watershed in the LVB of Uganda

3.4. Variation of Erosion Risk with Soil Type

Figure 5 presents predicted erosion risk obtained in the various soil units. The risk was highest in Lixic Ferralsols ($50 \text{ t ha}^{-1}\text{yr}^{-1}$), followed by Acric Ferralsols ($20 \text{ t ha}^{-1}\text{yr}^{-1}$), Arenosols ($15 \text{ t ha}^{-1}\text{yr}^{-1}$), Gleyic Arenosols ($2.5 \text{ t ha}^{-1}\text{yr}^{-1}$) and Planosols ($0 \text{ t ha}^{-1}\text{yr}^{-1}$). The high erosion rates predicted in the Lixic Ferralsols and Acric Ferralsols were unexpected since these soil units are generally not impacted by erosion. Although such soils have high iron content, they are associated with low plant nutrients, a strong acidity and low available phosphorus. The existence of a high soil loss risk among them is most likely a manifestation of poor management as well as the effect of slope gradient on runoff and soil loss. On Arenosols, a moderate soil loss risk observed was expected since these soils are generally infertile and so, they are undisturbed by agricultural activities providing a less potential for soil loss to occur. Coupled with this, a greater portion of the Arenosols in Nabajuzi watershed is being covered by grassland which protects them against erosive agents. A very low or nil soil loss risk was noted on the Gleyic Arenosols and Planosols since these were soil units mapped in the wetland area with a high potential for deposition.

3.5. Relationship between Soil Erosion Risk and Slope Angle in Nabajuzi Watershed

According to a previous study conducted in the LVB [24], this area is greatly affected by rill and interrill erosion. Premised on this idea, three important arguments relating slope angle and soil loss rates can be discussed. First is that soil loss is a power function of percent slope gradient, with exponents ranging between 0.7 and 2.0 [46].

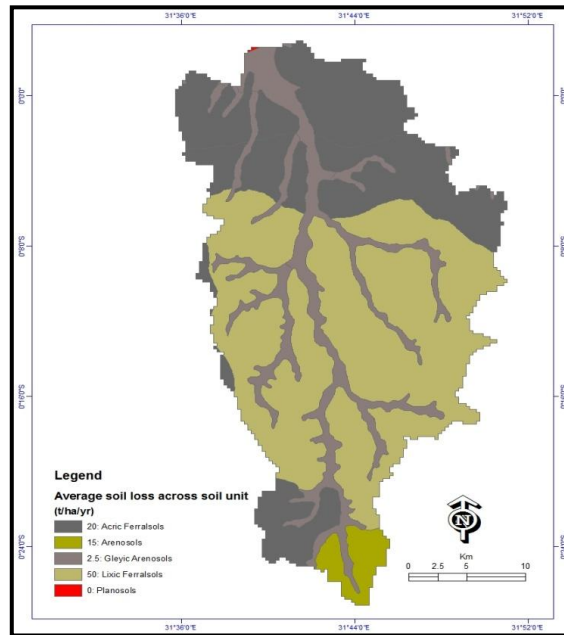


Figure 5: Variation of Soil Loss with Soil Type in Nabajuzi Watershed of LVB of Uganda

Second is that soil loss is a linear function of the sine of the slope gradient, with coefficients varying with slope gradient [27, 23]. Third is that soil loss is a polynomial function with the sine of slope gradient [45]. Yet, an earlier concern raised by [19] indicated that soil loss increases sharply with slope steepness until about 36%. But at steeper slopes which are greater than 86%, this curve relating slope steepness with soil loss rates flattens. Unfortunately, correlation coefficients to substantiate such claims at a watershed level are not readily available. In Nabajuzi watershed, slope percentages (Figure 6) were used to establish this coefficient of correlation between erosion risks and slope gradient. Potential erosion risk was highest (38–68) $t\ ha^{-1}yr^{-1}$ on the steepest slope gradient (15–18) %; and lowest (0–2.5) $t\ ha^{-1}yr^{-1}$ on the lowest slope gradient (0–5) %.

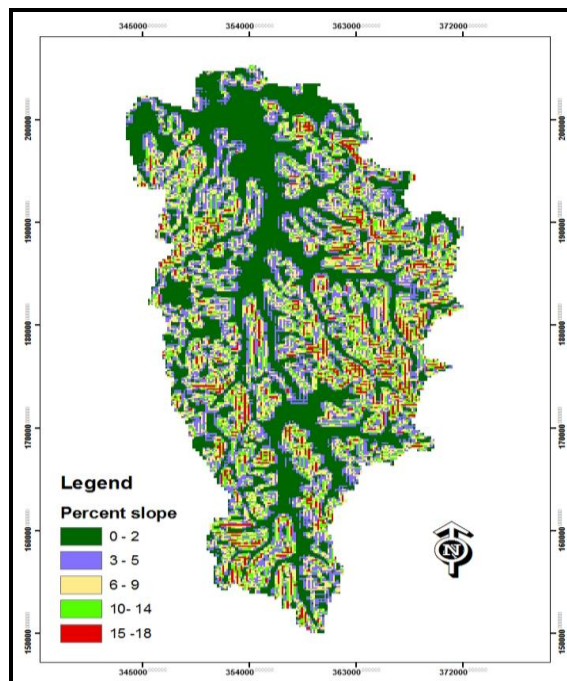


Figure 6: Slope Angle Categories in Nabajuzi Watershed of the LVB of Uganda

A strong linear relationship ($R= 0.96$) as in Figure 7, was recognized in this site; and soil erosion risk significantly varied with slope gradient ($P= 0.001$) at 95% significance level. This underscores the postulations by [19], [27] and by [23] as earlier discussed. Perhaps this observation is attributed to soil particle transport rather than to detachment processes; such that in absence of surface cover earlier highlighted by [40] for this watershed, runoff and soil loss increase with slope angle. A further empirical study investigating this issue is required in this watershed.

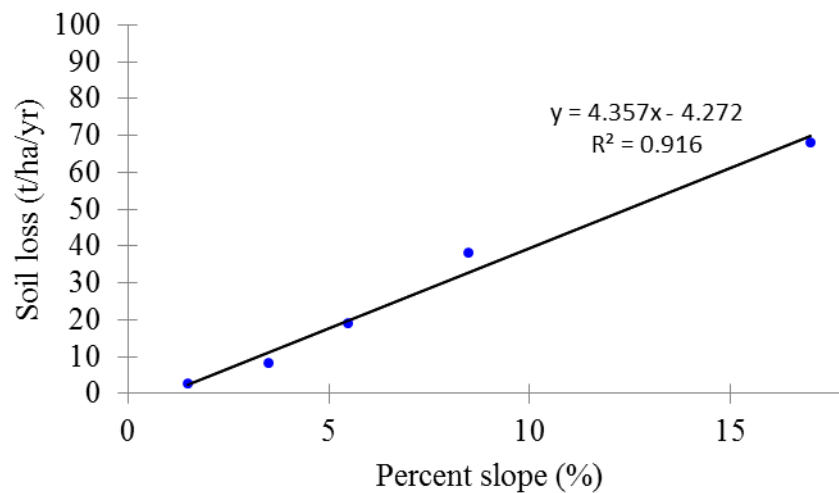


Figure 7: Correlating Slope Angle and Soil Loss in Nabajuzi Watershed in the LVB of Uganda

4. Conclusion

The predicted *LS* values derived by adapting RUSLE to C++ program had a strong linear correlation with the tabulated *LS* values. This C++ program expedites *LS* factor calculation particularly for a spatially heterogeneous watershed. This enables proper understanding of slope morphology and its related processes, thus fostering accurate erosion risk prediction at a large scale. Whereas the magnitude of erosion risk was generally moderate with respect to [11] rating, in some parts of Nabajuzi watershed a high risk potential was predicted. These areas require strategic maintenance for further reduction of soil erosion risk and restore the ecological functioning of Nabajuzi watershed of the LVB of Uganda.

Acknowledgement

We acknowledge research assistants and Sida Sarec (Swedish Research Grant) through Makerere University for partial funding.

References

- [1] Bagoora F.D.K., 1998: *Soil Loss in Rukiga Highlands in Eastern Kabale, Western Uganda*. Ph.D. Thesis, Makerere University, Kampala, Uganda.
- [2] Bamutaze Y., 2010: *Patterns of Water Erosion and Sediment Loading in Manafwa Catchment, Mt. Elgon, Eastern Uganda*. Ph.D. Thesis, Makerere University, Kampala, Uganda.
- [3] Bols P., 1978: *The Iso-erodent Map of Java and Madura*. Belgian Technical Assistance Project ATA 105, Soil Research Institute, Bogor.

- [4] De Baets S., Poesen J., Meersmans J. and Serlet L. *Cover Crops and Their Erosion-Reducing Effects during Concentrated Flow Erosion*. Catena. 2011. 85; 237-244.
- [5] De Baets S., Poesen J., Gyssels G., and Knapen A. *Effects of Grass Roots on the Erodibility of Top Soils during Concentrated Flow*. Geomorphology. 2006. 76; 54-67.
- [6] Desmet P. and Grovers G. *GIS-Based Simulation of Erosion and Deposition Patterns in an Agricultural Landscape: A Comparison of Model Results with Soil Map Information*. Catena. 1995. 25; 389-401.
- [7] Desmet P. and Grovers G. *A GIS Procedure for Automatically Calculating the USLE LS Factor on Topographically Complex Landscape Units*. Journal of Soil and Water Conservation 1996. 51 (5) 427-433.
- [8] Derpsch R. and Friedrich T., 2009: *Global Overview of Conservation Agriculture Adoption Proceedings*. Lead Paper, 4th World Congress on Conservation Agriculture, New Delhi, India. 429-438.
- [9] El-Hassanin A.S., Labib T.M. and Gaber E.I. *Effect of Vegetation Cover and Landscape on Runoff and Soil Losses from Watersheds of Burundi*. Agricultural Ecosystems and Environment. 1993. 43; 301-308.
- [10] El-Swaify S.A. *Factors Affecting Soil Erosion Hazards and Conservation Needs for Tropical Steep Lands*. Soil Technology. 1997. 11; 3-16.
- [11] Food and Agriculture Organization (FAO), 1990. FAO Yearbook 1989. Production, FAO Statistical Series No. 94, Vol. 43, FAO Rome, Italy.
- [12] Foster G.R., Lane L.J., Nowlin J.D., Laflen J.M. and Young R.A. *Estimating Erosion and Sediment from Field-Sized Area*. Transactions ASAE. 1981. 24; 1253-1262.
- [13] Griffin M.L., Beasley D.B, Fletcher J.J. and Foster G.R. *Estimating Soil Loss on Topographically Non-Uniform Field and Farm Units*. Journal of Soil and Water Conservation. 1988. 43; 326-331.
- [14] Ha N.T., 1996: *Definition of the Affected Factors to Soil Erosion and Prediction of Soil Loss in the Sloped Area*. Ph.D. Thesis, Hanoi University of Irrigation Science.
- [15] Halim R., Clemente R.S., Routray J. K. and Shrestha R.P. *Integration of Bio-Physical and Socio-Economic Factors to Assess Soil Erosion Hazard in the Upper Kaligarang Watershed, Indonesia*. Land Degradation and Development. 2007. 18; 453-469.
- [16] Harrop J.F., 1970: *The Soils of the Western Provinces of Uganda, Memoirs of the Research Division*. Series 1- Soils, No. 6, Department of Agriculture, Uganda.
- [17] Hickey R. Slope Angle and Slope Length Solutions for GIS. Cartography. 2000. 29 (1) 1-8.
- [18] Hickey R., Smith A. and Jankowski P. *Slope Length Calculations from a DEM within Arc/Info GRID*. Computers, Environment and Urban Systems. 1994. 18 (5) 365 - 380.
- [19] Horton R.E. *Erosional Development of Streams and their Drainage Basins: Hydrological Approach to Quantitative Morphology*. Geographical Society of America, Bulletin. 1945. 56; 275-370.

- [20] Hussein M.H. *An Analysis of Rainfall, Runoff and Erosion in the Low Rainfall Zone of Northern Iraq*. Journal of Hydrology. 1996. 181; 105-126.
- [21] Lal R. *Soil Science and Carbon Civilization*. Soil Science Society of America Journal. 2007. 71; 1425-1437.
- [22] Lillesand T.M. and Kiefer R.W., 1994: *Remote Sensing and Image Interpretation*. 3rd Ed., Wiley.
- [23] Liu B.Y., Nearing M.A. and Risse L.M. Slope Gradient Effects on Soil Loss for Steep Slopes. Transactions of America Society of Agriculture Engineers (ASAE). 1994. 37 (6) 1835-1840.
- [24] Lufafa A., Tenywa M.M., Isabirye M., Majaliwa M.J.G. and Woomeer P.L. *Prediction of Soil Erosion in a Lake Victoria Basin Catchment Using GIS-Based USLE Model*. Agricultural Systems. 2003. 76 (3) 883-894.
- [25] Majaliwa M.G.J., 2005: Soil Erosion from Major Agricultural Landuse types and Associated Pollution Loading in Selected Lake Victoria Micro-Catchments. Ph.D. Thesis, Makerere University, Kampala, Uganda.
- [26] Mamo M. and Bubenger G.D. *Detachment Rate, Soil Erodibility and Soil Strength as Influenced by Plant Roots: Laboratory and Field Study (Part 1 and 2)*. Transactions of American Society of Agricultural Engineers. 2001. 44; 1167-1187.
- [27] McCool D.K., Brown L.C., Foster G.R., Mutchler C.K. and Meyer L.D. *Revised Slope Steepness Factor for the Universal Soil Loss Equation (USLE)*. Transactions of America Society of Agriculture Engineers (ASAE). 1987. 30 (5) 1387-1396.
- [28] Mitasova H. *Surfaces and Modeling*. Grass Clippings. 1993. 7 (1) 18-19.
- [29] Mitasova H., Hofierka J., Zlocha M. and Iverson L. *Modeling Topographic Potential for Erosion and Deposition using GIS*. International Journal of GIS. 1996. 10 (5) 629-641.
- [30] Moore R.R. *Rainfall Erosivity in East Africa: Kenya, Tanzania and Uganda*. Geografika Annaler. Series A. Physical Geography. 1979. 61; 147-156.
- [31] Moore I.D. and Wilson J.P. *Length-Slope Factors for the Revised Universal Soil Loss Equation (RUSLE): Simplified Method of Estimation*. Journal of Soil and Water Conservation. 1992. 47 (5) 423-428.
- [32] NRCS-USDA, 2002: *Technical Guide to RUSLE use in Michigan, State Office of Michigan*. Institute of Water Research, Michigan State University. www.iwr.msu.edu/rusle/lstable.htm.
- [33] Renard K.G., Foster G.R., Weesies G.A., McCool D.K., and Yoder D.C., 1997. *Predicting Soil Erosion by Water: Guide to Conservation Planning with the Revised Universal Soil Loss Equation (RUSLE)*. Agricultural Hand Book, Vol. 703. US Department of Agriculture, Washington, DC, USA. 1-251.
- [34] Renard K., G.R. Foster, G.A. Weesies and J.P. Porter. *RUSLE Revised Universal Soil Loss Equation*. Journal of Soil and Water Conservation. 1991. 46; 30-33.

- [35] Renschler C.S. and Harbor J. *Soil Erosion Assessment Tools from Point to Regional Scales-the Role of Geomorphologists in Land Management Research and Implementation*. *Geomorphology* 2002. 47; 189-209.
- [36] Shi Z.H., Cai C.F., Ding S.W., Wang T.W., and Chow T.L. *Soil Conservation Planning at Small Watershed Level Using RUSLE with GIS: A Case Study In Three Gorge Area of China*. *Catena*. 2004. 55; 33-48.
- [37] Sinun W., Wong W.M., Douglas I. and Spencer T., 1992: *Through Fall, Stem Flow, Overland Flow and Through Flow in the Ulu Segaman Rain Forest, Sabah*. *Phil. Transactions of the Royal Society, London, UK*, B335-389-395.
- [38] Srinivasan R. and Engel B.A. *Effect of Slope Prediction Methods on Slope and Erosion Estimates*. *Applied Engineering in Agriculture*. 1991. 76 (6) 779-783.
- [39] Styczen M.E. and Morgan R.P.C., 1995: *Engineering Properties of Vegetation*. In: Morgan, R.P. C., Rickson, R.J., Eds. *Slope Stabilization and Erosion Control: A Bioengineering Approach*: E and F.N. Spon, London, 5-58.
- [40] Tenywa M.M., Isabirye M.I., Lal R., Lufafa A., and Achan P. *Cultural Practices and Production Constraints in Smallholder Banana-Based Cropping of Uganda's Lake Victoria Basin*. *African Crop Science Journal*. 1999. 7 (4) 541-550.
- [41] Van Remortel R., Maichle R. and Hickey R. *Computing the RUSLE LS Factor Based on Array-Based Slope Length Processing of Digital Elevation Data Using a C++ Executable*. *Computers and Geosciences*. 2004. 30 (9/10) 1043-1053.
- [42] Wischmeier W.H. and Smith D.D., 1965: *Predicting Rainfall Erosion Losses from Crop Land East of the Rocky Mountains: A Guide for Selection of Practices for Soil and Water Conservation*. Agriculture, Washington, DC, USA.
- [43] Wischmeier W.H. and Smith D.D., 1978: *Predicting Rainfall Erosion Losses*. US Department of Agriculture (USDA), Agricultural Research Service, Hand Book No. 537, 58.
- [44] Wu W.D., Zheng S.Z. and Lu Z.H. *Effect of Plant Roots on Penetrability and Anti-Scourability of Red Soil Derived from Granite*. *Pedosphere*. 2000. 10; 183-188.
- [45] Zhang K.L. and Hosoyamada K. *Influence of Slope Gradient on Interrill Erosion of Shirasu Soil*. *Soil Physical Conditions and Plant Growth in Japan*. 1996. 73; 37-44.
- [46] Zhang X.C., Nearing M.A., Miller M.P., Norton L. and West L.T. *Modelling Interrill Sediment Delivery*. *Soil Science Society of America Journal*. 1998. 62 (2) 438-444.
- [47] Zhang H., Yang Q., Li R., Liu Q., Moore D., He P., Ritsema C. J., and Geissen V. *Extension of a GIS Procedure for Calculating the RUSLE Equation LS Factor*. *Computers and Geosciences*. 2013. 52; 177-188.
- [48] Zhou Z.C. and Shangguan Z.P. *The Effects of Ryegrass Roots and Shoots on Loess Erosion under Simulated Rainfall*. *Catena*. 2007. 70; 350-355.